[American Journal of Science, Vol. 313, December, 2013, P. 1054–1087, DOI 10.2475/10.2013.04]

JURASSIC OPHIOLITE FORMATION AND EMPLACEMENT AS BACKSTOP TO A SUBDUCTION-ACCRETION COMPLEX IN NORTHEAST TURKEY, THE REFAHİYE OPHIOLITE, AND RELATION TO THE BALKAN OPHIOLITES

GÜLTEKİN TOPUZ*,†, Ö. FARUK ÇELİK**, A. M. CELÂL ŞENGÖR*, İ. EMİR ALTINTAŞ*, THOMAS ZACK***, YANN ROLLAND§, and MATHIAS BARTH§§

ABSTRACT. The eastern Mediterranean region within the Tethyan realm shows a high concentration of ophiolites with contrasting times of formation and emplacement along the belt: In the Balkans, the ophiolites formed during the early to medial Jurassic, and were obducted during the late Jurassic, whereas in Turkey and farther east, structurally intact Jurassic ophiolites are rare and Jurassic ophiolite obduction is unknown. Here we report a structurally intact, large ophiolite body of early Jurassic age from NE Turkey, the Refahiye ophiolite, located close to the suture zone between the Eastern Pontides and the Menderes-Taurus block. The Refahiye ophiolite forms an outcrop belt, 175 km long and 20 km wide, and is tectonically bound by the late Cretaceous ophiolitic mélange to the south, and by the North Anatolian Transform Fault against the Triassic low-grade metamorphic rocks to the north. Early to medial Jurassic very low- to low-grade metamorphic rocks, interpreted as intraoceanic subduction-accretion complexes, occur either beneath the ophiolite or as thrust slices within it. The ophiolite body within the studied section is made up of mantle peridotite (clinopyroxene-bearing harzburgite and minor dunite) crosscut by up to 20 cm thick veins of clinopyroxenite and later dikes/pods/stocks of gabbro ranging in size from 2 m to several hundreds of meters. The gabbro is represented by two distinct types: (i) cumulate gabbro, and (ii) non-cumulate gabbro with locally well-developed igneous foliation. Within the non-cumulate gabbro or enclosing peridotite, there are up to 5 m and 50 cm-thick veins of trondhjemite and pegmatitic gabbro, respectively. LA-ICP-MS dating on zircons from two trondhjemite samples yielded weighted mean ages of ~184 ± 4 Ma and 178 ± 4 Ma (2σ), respectively, suggesting formation during early Jurassic time. Formation in a suprasubduction-zone forearc setting is inferred from (i) wide-ranging pyroxene and spinel compositions in the peridotites as documented in most suprasubduction-zone ophiolites, (ii) arc tholeiitic signature of the non-cumulate gabbros, and (iii) association of the ophiolite with the coeval subduction-accretion complexes. Emplacement of a trapped forearc ophiolite above its own subduction-accretion complex as a backstop is proposed based on a series of field relationships such as (i) intimate association of the unsubducted suprasubduction-zone ophiolite with coeval accretionary complexes, (ii) absence of unambiguous relationship to the southern Atlantic-type continental margin, and (iii) absence of any stratigraphic indications for the ophiolite obduction in the southern Atlantic-type continental margin during Jurassic time. This is a clear difference from the Jurassic ophiolites in the Balkans that were obducted over the Atlantic-type continental margin. This difference in mode of emplacement is most probably related to the greater distance of the intra-oceanic subduction zone to the Atlantic-type continental margin than it was in the Balkans, which is commensurate with the greater width of the Tethys in the east during Jurassic time.

* Istanbul Teknik Üniversitesi, Avrasya Yer Bilimleri Enstitüsü, Ayazağa TR80626, Istanbul, Turkey
** Kocaeli Üniversitesi, Jeoloji Mühendisliği Bölümü, Umuttepe Yerleşkesi, TR41380 Kocaeli, Turkey
*** Department of Earth Sciences, University of Gothenburg, 40530 Gothenburg, Sweden
§ Géoazur, Université de Nice-Sophia Antipolis, OCA, CNRS, 250 rue A. Einstein, Sophia Antipolis 06560 Valbonne, France
§§ Institut für Geowissenschaften, Universität Mainz, Johann-Joachim-Becher Weg 21, 55099 Mainz, Germany
† Corresponding author: topuzg@itu.edu.tr

Key words: Suprasubduction, ophiolite emplacement, Eastern Pontides, Balkan ophiolites, Jurassic, Turkey

INTRODUCTION

Ophiolites have long been recognized as fragments of oceanic crust and upper mantle on or in continental crust that, if not transported over large distances from their original site of incorporation into the continent, delineate accretionary belts or suture zones between formerly separate continents (Coleman, 1971; Dewey and Bird, 1971; Dewey, 1976, 2003; Moores, 1982; Shervais, 2001; Wakabayashi and Dilek, 2003). The central problems of ophiolite studies have been the obduction of ophiolites, particularly large, intact pieces of oceanic crust and mantle over less dense continental crust or into/onto accretionary complexes, and its episodic nature. It is argued that the ophiolite obduction is related to plate acceleration brought about by plate reorganization (for example, Agard and others, 2007). Mainly two distinct modes of ophiolite emplacement are differentiated (compare Moores, 1982; Wakabayashi and Dilek, 2000, 2003; Şengör and Natal'in, 2004): (i) obduction of large ophiolite nappes over the Atlantic-type continental margins, and (ii) emplacement to or onto Pacific-type continental margins. During the emplacement onto Atlantic-type continental margins, ophiolite is thrust over the passive margin by exploiting the downbending of the margin, as the subduction zone converges onto the margin, as documented in most Tethyan ophiolites (for example, Şengör, 1990; Okay and others, 2001; Robertson, 2006; Robertson and others, 2009). The emplacement to or onto Pacific-type continental margins can occur in several different ways such as (i) forming backstops to accretionary complexes, (ii) wedging into subduction-accretion complexes of ophirags (smaller fragments of oceanic lithosphere, see Dewey, 2003; Şengör and Natal'in, 2004) or large sheets of ophiolites, or (iii) backthrusting of ophirags or even more complete ophiolite nappes onto arc units of Pacific-type continental margins. *In forming backstops to accretionary complexes,* large sheets of oceanic lithosphere structurally overlies subduction-accretion complex as in the Coast Range ophiolite in California (Stern and Bloomer, 1992; Wakabayashi and Dilek, 2000, 2003; Shervais, 2001; Wakabayashi and others, 2010), the Border Range ophiolite in Alaska (Kusky and others, 2007), and Sangilen, North Sayan and West Sayan ophiolites of the Altaids (Şengör and Natal'in, 2004). Accretion of oceanic material beneath ophiolite in the subduction zone leads to gradual elevation until buoyancy exhumes high pressure metamorphic rocks. *In wedging into the subduction-accretion complexes,* the ophirags or large sheets of ophiolites were either scraped off subducting plates or derived from the overlying forearc ophiolite, as happened in the Franciscan complex (Coleman, 2000; Şengör and Natal'in, 2004; Wakabayashi, 2013). *In the backthrusting of ophirags or even more complete ophiolite nappes onto arc units of Pacific-type continental margins,* rears of the accretionary wedges are backthrusted onto forearc basins due to anomalous stress conditions built across the accretionary wedge and overlying suprasubduction-zone ophiolite during ongoing subduction or collision (for example, Bergougnan, 1975, ms 1986; Hamilton, 1979; Karrig and others, 1980; Şengör and Yılmaz, 1981; Westbrook, 1982; Silver and Reed, 1988). Overall, timing of ophiolite genesis and its mode of emplacement provide important constraints on intra-oceanic subduction processes, and growth of orogenic belts, respectively.

The eastern Mediterranean region within the Tethysides is characterized by a amount of ophiolites and ophirags (Şengör and Yılmaz, 1981; Şengör, 1990; Şengör and Natal'in, 1996; Okay and others, 2001; Robertson, 2002, 2006, 2012; Robertson and others, 2009). The structurally intact large ophiolite bodies display contrasting spreading ages and timing of emplacement (fig. 1): From west to east, ages of the ophiolites are early to medial Jurassic in the Eo-Hellenic nappes in the Balkans (for example, Bernoulli and Laubscher, 1972; Lanphere and others, 1975; Roddick and

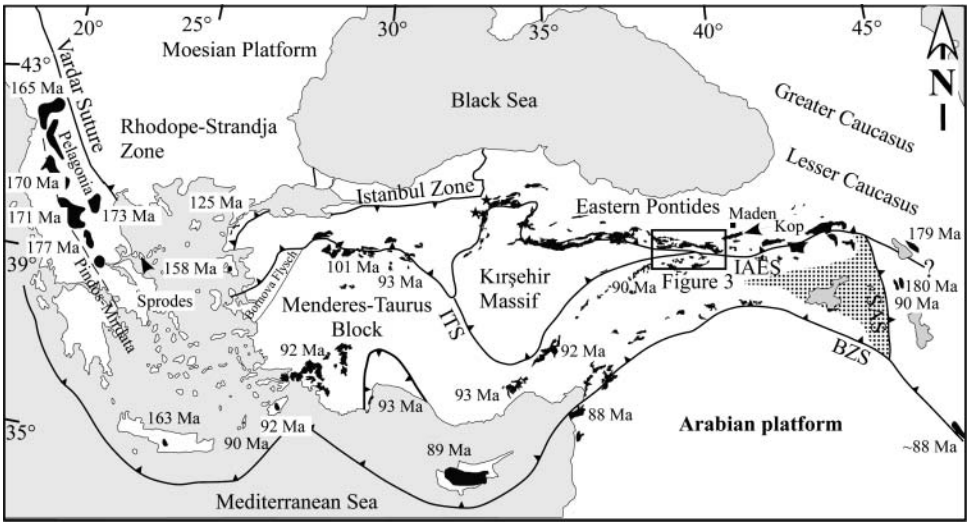

Fig. 1. Main tectonic blocks in the Eastern Mediterranean region (modified after Şengör and Yılmaz, 1981; Okay and Tüysüz, 1999). Dotted domain stands for the Eastern Anatolian accretionary complex. IAES: Izmir-Ankara-Erzincan suture; ITS: Inner Tauride suture; SAS: South Azerbaijan suture; BZS: Bitlis-Zagros suture. The exact boundary cannot be determined due to extensive young volcanic cover. The black domains show the main ophiolites together with radiometric ages. Stars stand for the locations of Jurassic ophirags in the Cretaceous ophiolitic mélanges (Dilek and Thy, 2006; Çelik and others, 2011, 2013; Göncüoğlu and others, 2012).

others, 1979; Spray and others, 1984; Jacobshagen, 1986; Hatzipanagiotou and Pe-Piper, 1995; Dimo-Lahitte and others, 2001; Koepke and others, 2002; Liati and others, 2004), late Cretaceous in Turkey, Cyprus and Syria (for example, Harris and others, 1994; Dilek and Whitney, 1997; Dilek and others, 1999; Parlak and Delaloye, 1999; Önen and Hall, 2000; Önen, 2003; Çelik and others, 2006; Chan and others, 2007; Dilek and Thy, 2009; Parlak and others, 2013a), early to medial Jurassic in the Lesser Caucasus (Galoyan and others, 2009; Rolland and others, 2009a, 2010; Hassig and others, 2013). Evidence for the Jurassic oceanic spreading in Turkey comes exclusively from the Jurassic ophirags or blocks of ophiolite-related metamorphic rocks within the Cretaceous ophiolitic mélanges (Dilek and Thy, 2006; Çelik and others, 2011, 2013; Göncüoğlu and others, 2012). Emplacements of the ophiolites over Atlantic-type continental margins occurred during late Jurassic in the Balkans, late Cretaceous in Turkey, Syria, and the Lesser Caucasus (Şengör, 1990; Şengör and Natal'in, 1996; Okay and others, 2001; Robertson, 2004; Robertson and others, 2009; Sosson and others, 2010). Causes of the rarity of the structurally intact large Jurassic ophiolites and the absence of Jurassic obduction over the Atlantic-type margins in Turkey and farther east in clear contrast to the Balkans have so far been unclear.

The present paper presents one possible solution to this long-standing problem of not having any Jurassic obduction in Turkey, in which we present field geological, geochemical and geochronological data on a large ophiolite body, the Refahiye ophiolite, from the Eastern Pontides (northeast Turkey), and discuss these data in the context of ophiolite formation and emplacement in the Eastern Mediterranean region. Our data together with the critical assessment of the literature clearly show that (i) the Refahiye ophiolite formed during the early Jurassic in a suprasubduction-zone forearc setting, and (ii) was emplaced over its own subduction-accretion complex at the Pacific-type continental margin of the Eastern Pontides.

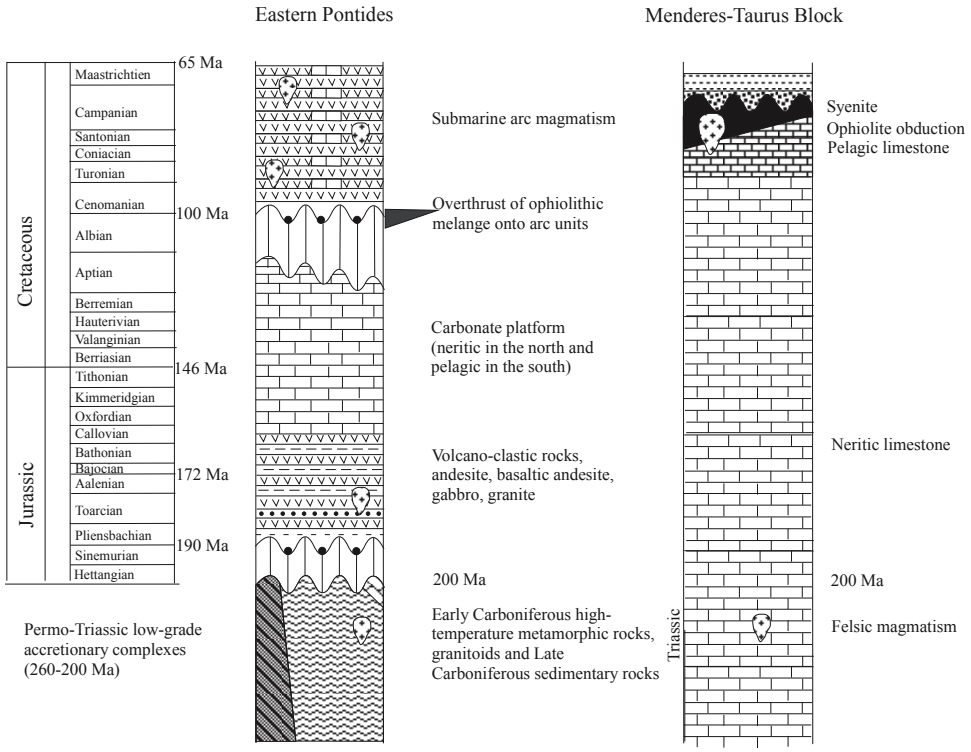

Fig. 2. Regional stratigraphic columnar sections of the Eastern Pontides and Menderes-Taurus block. Geological time scale is from Ogg and others (2008).

GEOLOGICAL SETTING

The Eastern Mediterranean Alpides are made up of a number of continental blocks separated by sutures (fig. 1) (Şengör and Yılmaz, 1981; Şengör and Natal'in, 1996; Okay and Tüysüz, 1999; Moix and others, 2008). The Izmir-Ankara-Erzincan suture (IAES) in northern Turkey separates the continental blocks of the composite Pontides (Rhodope-Strandja, Istanbul Zone, Eastern Pontides) in the north and the Menderes-Taurus block and the Kırşehir Massif in the south. The Eastern Pontides and Menderes-Taurus block display striking differences in their pre-Paleocene stratigraphy (fig. 2). The IAES represents the trace of an oceanic domain dating back to Devonian times, and was consumed by northward subduction under the Pontides from late Paleozoic to end-Mesozoic with continental collision during Paleocene–early Eocene (Ustaömer and Robertson, 2010; Topuz and others, 2011, 2013a).

The pre-Jurassic basement of the Eastern Pontides consists of (i) a Carboniferous domain with high-temperature/low-pressure metamorphic rocks, high-K I-type granites, and sedimentary rocks (fig. 2) (Şengör and Yılmaz, 1981; Okay and Leven, 1996; Topuz and others, 2004a, 2007, 2010; Dokuz, 2011; Kaygusuz and others, 2012; Ustaömer and others, 2013), and (ii) Permo-Triassic low-grade oceanic accretionary complexes, commonly known as the Karakaya complex (Şengör and others, 1980; Okay, 1984; Topuz and others, 2004b, 2013b). Both are unconformably overlain by a Lower to Middle Jurassic transgressive volcanoclastic series including local ammonnitico-rosso horizons with local coeval gabbro, diorite and I-type granite (for example, Görür and others, 1983; Yılmaz and Boztuğ, 1986; Konak and others, 2001; Şen, 2007;

Kandemir and Yılmaz, 2009; Genç and Tüysüz, 2010; Dokuz and others, 2010; Ustaömer and Robertson, 2010; Ustaömer and others, 2013), grading conformably into late Jurassic to early Cretaceous platform carbonates with sporadic early Cretaceous magmatism (Pelin, 1977; Boztuğ and Harlayan, 2008; Koch and others, 2008). There is a local unconformity between the Lower and Upper Cretaceous rocks (Görür and others, 1993). During the late Cretaceous, voluminous submarine arc magmatism on the entire Pontides resumed (Şengör and Yılmaz, 1981; Okay and Şahintürk, 1997). An outstanding feature of the Eastern Pontides is that an early Cretaceous ophiolitic mélange is overthrust onto forearc units up to distances ≤100 km from the IAES (fig. 3A) (Bergougnan, 1975, ms 1986; Şengör and Yılmaz, 1981; Okay and Şahintürk, 1997). An early Cretaceous age is assigned to the ophiolitic mélange, because ages of the limestone blocks in the mélange range up to the Albian. This ophiolitic mélange is locally unconformably overlain by Maastrichtian reefal limestone in the Maden area (fig. 1), placing a lowest age constraint on the overthrust (Okay and Şahintürk, 1997). The northward overthrust of the ophiolitic mélange was ascribed to retrocharriage at the contact between the arc and accretionary wedge by Şengör and Yılmaz (1981), and was probably concurrent with the Cenomanian uplift in the Eastern Pontides, because it represents the only compression period during Cretaceous time (Şengör and Yılmaz, 1981; Okay and Şahintürk, 1997).

The Menderes-Taurus block[1] forms the easternmost extension of the Apulia, and has a possibly Archaean (Kröner and Şengör, 1990) to Late Proterozoic to Early Cambrian crystalline basement overlain by Paleozoic and Mesozoic sedimentary successions with some Triassic igneous activity (fig. 2) (Şengör and others, 1984; Özgül and Turşucu, 1984; Koralay and others, 2001; Candan and others, 2011; Akal and others, 2012). From Triassic to Late Cretaceous time, the Menderes-Taurus block was characterized mostly by the deposition of neritic limestones concordantly overlain by Turonian to Campanian pelagic equivalents in the north and central parts. Before the medial Campanian, large ophiolite nappes together with underlying ophiolitic mélanges were obducted over the leading edge of the Menderes-Taurus block (fig. 3) (Ricou and others, 1975; Şengör and Yılmaz, 1981; Özgül and Turşucu, 1984; Okay and Şahintürk, 1997; Rice and others, 2006, 2009; Robertson and others, 2009), deducted from (i) the "Campanian" age of the uppermost part of the Munzur limestone sequence, (ii) intrusion of the ophiolite and the underlying limestone by syenite as old as ~67 to 70 Ma (Parlak and others, 2013a), and (iii) change from neritic carbonate deposition to a pelagic one most likely because of the isostatic effects of the ophiolite obduction.

The IAE suture between the composite Pontides and Menderes-Taurus block is marked by large tracts of ophiolite, low-grade metamorphic rocks and late Cretaceous ophiolitic mélanges (figs. 1 and 3). From the regional geological constraints described above, it is apparent that there are temporally and spatially distinct ophiolites and ophiolitic mélanges: (i) An early Cretaceous ophiolitic mélange overthrust onto the forearc units of the Eastern Pontides, (ii) ophiolite with underlying ophiolitic mélange obducted onto the northern edge of the Menderes-Taurus block, represented by Munzur limestone, and (iii) large ophiolite tracts in tectonic contact with low-grade

[1] Originally Şengör and Yılmaz (1981) incorporated the Taurus mountains—including the Munzurs, the Malatya metamorphics and the Pötürge and Bitlis massifs—the Menderes massif and the Kırşehir massif into a single Anatolide-Tauride continental fragment forming a direct easterly continuation of the Apulian platform. In 1982, Şengör and others recognized that the Kırşehir massif was separated from the rest by a suture zone, called the Inner Tauride suture. Since then the easternmost end of the Apulian platform has been called the Menderes-Taurus block to underline that the Kırşehir, a part of Ketin's (1966) Anatolides, is no longer a part of the palaeotectonic units including the Taurus mountains and the Menderes massif. However, some authors continued to use the now-incorrect term Anatolide-Tauride block.

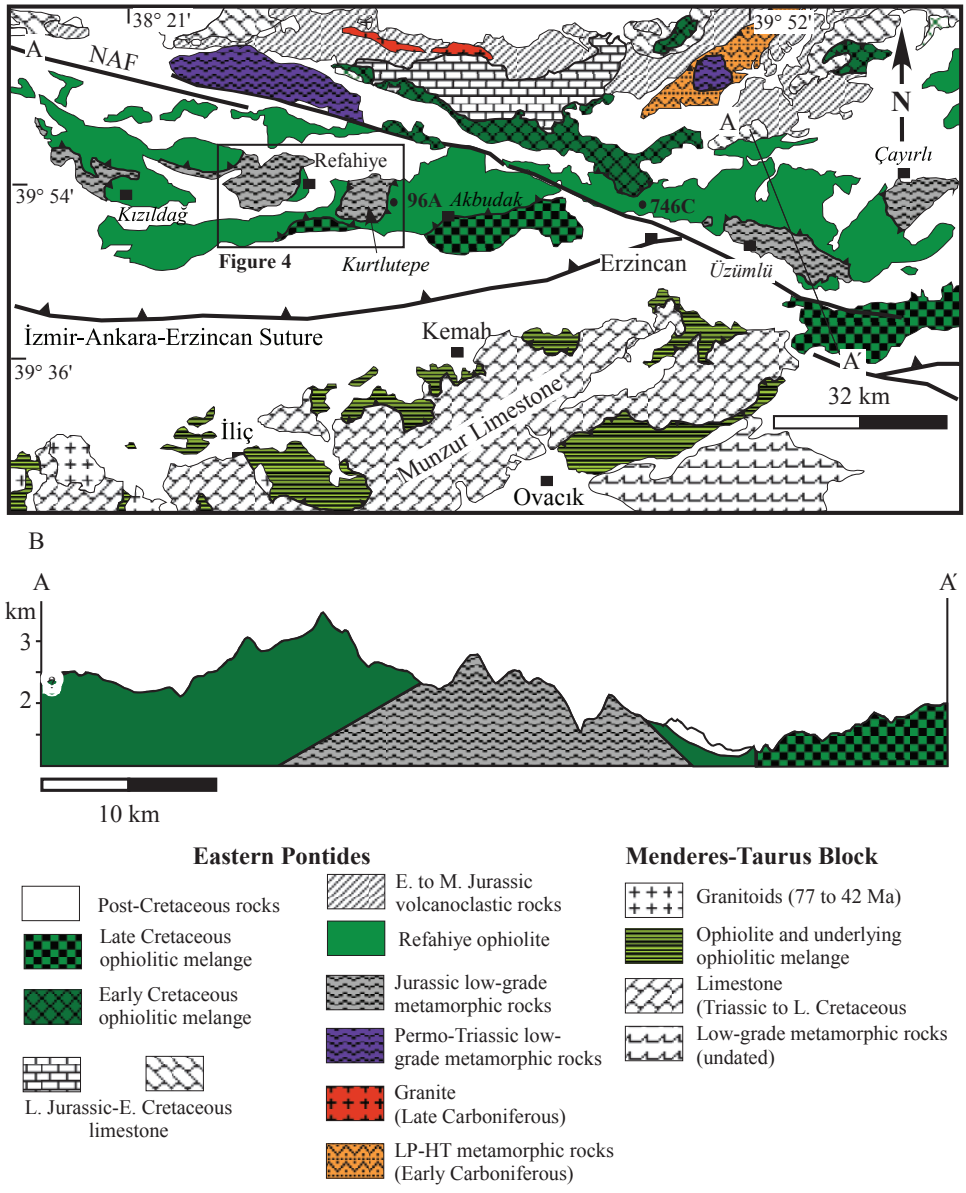

Fig. 3. (A) Geological map of the Refahiye ophiolite (modified after Akbaş and others, 2011). NAF stands for the North Anatolian Fault, (B) Cross-section across A-A′ line.

(for example, greenschist to blueschist-facies) metamorphic rocks, and late Cretaceous ophiolitic mélanges (Topuz and others, 2013a).

THE REFAHİYE OPHIOLITE AND ASSOCIATED METAMORPHIC ROCKS

The Refahiye ophiolite, cropping out in an area ~175 km long and up to 20 km wide, is located in the Eastern Pontides close to the IAE suture (fig. 3A) (Yılmaz, 1985; Yılmaz and Yılmaz, 2004; Rice and others, 2006, and 2009; Sarıfakıoğlu and others,

2009; Parlak and others, 2013b). To the south, the ophiolite body is tectonically underlain by the late Cretaceous ophiolitic mélange, consisting of blocks of basalt, radiolarian chert, pelagic and neritic limestone, shale, serpentinized peridotite, blueschist, amphibolite and mica schist. The NW-SE trending North Anatolian fault (NAF) here with a lateral offset of ~60 to 85 km (Şengör and others, 2005) bisects the Refahiye ophiolite: In the western part of the ophiolite, the NAF bound the Refahiye ophiolite against the Ağvanis massif which is made up of late Triassic greenschist- to albite-epidote-amphibolite-facies metabasite, marble, phyllite, and subordinate serpentinite and metachert (Okay, 1984; Topuz and others, 2013b). To the east of the NAF, early Cretaceous ophiolitic mélange tectonically rests over the northern part of the Refahiye ophiolite. The ophiolite is tectonically associated with the low-grade metamorphic rocks of early to medial Jurassic age, cropping out at five isolated localities such as Çayırlı, Üzümlü, Kurtlutepe, Refahiye and Kızıldağ from east to west (figs. 3A and 3B). The metamorphic rocks either tectonically underlie the ophiolite as in the Çayırlı, Üzümlü, and Kızıldağ areas, or are interleaved with it as in the Kurtlutepe and Refahiye areas, and do not have any direct contact relationship with the southern late Cretaceous ophiolitic mélange. The contacts with the interleaved metamorphics are represented mainly by low-angle faults apart from the easternmost contact of the Kurtlutepe domain. Both the ophiolite and metamorphic rocks are unconformably overlain by medial Eocene and younger clastic sedimentary rocks, placing a minimum age constraint for the tectonic interleaving. Based on the age of the oldest unconformably overlying sedimentary rocks, a late Cretaceous spreading age is generally assumed for the Refahiye ophiolite in previous studies (Yılmaz, 1985; Yılmaz and Yılmaz, 2004; Rice and others, 2006, 2009; Sarıfakıoğlu and others, 2009; Parlak and others, 2013b), although the possibility of formation during the Jurassic was not totally excluded. Yet, Uysal and others (2010) infer a Late Carboniferous formation age on the basis of Re-Os whole rock dating for the Refahiye ophiolite.

In this study, we mapped at a scale of 1/25,000 an area 720 km^2, 36 km by 20 km, including the Refahiye and Kurtlutepe metamorphic domains (fig. 4A). In the studied transect, overall the ophiolite lacks obvious signs of regional metamorphism, and is represented by mantle peridotite (clinopyroxene-bearing harzburgite with minor dunite and chromite deposits), locally crosscut by up to 30 cm thick dikes of clinopyroxenite and gabbroic intrusions postdating the clinopyroxenite dikes, ranging in size from a few meters to several hundreds of meters (figs. 5A and 5B). The gabbroic rocks are of two distinct types: (i) A layered gabbroic stock (type-I), only exposed from the west of the Refahiye town, (ii) non-cumulate gabbroic rocks (type-II). The type-II gabbroic rocks form numerous dikes/pods/stocks. Some dikes cross-cut others, suggesting multiple dike emplacements. Within type-II gabbros and hosting peridotite, there are ≤50 cm-thick discontinuous veins of trondhjemite (fig. 5C) and pegmatitic gabbro. Overall, serpentinization and carbonatization are widespread in the peridotite. Nearly 65 km to the east of the study area, from the north of Erzincan (fig. 3A), Sarıfakıoğlu and others (2009) and Parlak and others (2013b) describe domains of cumulate peridotite-gabbro, isotropic gabbro and sheeted dike complex in addition to the mantle peridotite.

The Refahiye metamorphic rocks consist of predominantly greenschist (~40 % of the outcrop area), marble (~30 %), serpentinite (~20 %), phyllite (~10 %), and minor metachert, amphibolite, garnet amphibolite, eclogite and garnet mica schist. Amphibolite, garnet amphibolite, eclogite and garnet micaschist termed "high-grade blocks," are encountered in two locations with sizes up to 10 m (indicated by stars in fig. 4A). Greenschist contains actinolite/Na-Ca amphibole, epidote, chlorite, albite, titanite, ±phengite, ±calcite ±quartz and ±hornblende and ±rutile. Hornblende and rutile occur locally in some samples, and are replaced by actinolite and titanite,

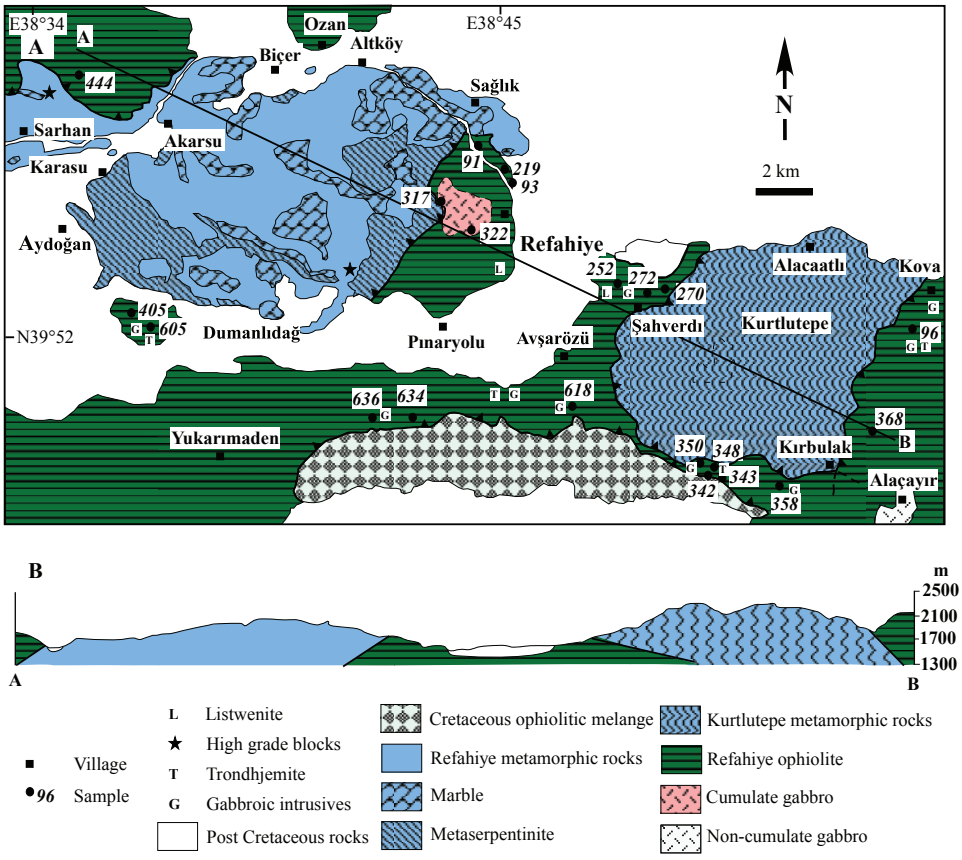

Fig. 4. (A) Geological map together with the sample locations (see fig. 3 for location), (B) Cross-section across A-B line.

respectively. Phyllite includes mineral assemblages involving quartz, muscovite-phengite, chlorite, albite, rutile, ±garnet, ±tourmaline and ±stilpnomelane. Common presence of relict phases (such as rutile, hornblende) and chlorite pseudomorphs after garnet suggest that "at least" parts of the greenschist-facies rocks represent the retrograded products of garnet-amphibolite and eclogite-facies metamorphism. Stepwise Ar-Ar dating of white micas from two phyllite samples and U-Pb rutile dating of rutile from a mica schist sample consistently yielded ages of 175 ± 5 Ma (2σ), suggesting that the metamorphism occurred during the early to medial Jurassic (Topuz and others, 2013a). Due to widespread presence of oceanic rock types (serpentinite, metachert) and overall absence of any granitic rocks, the rock assemblage was interpreted as an oceanic subduction-accretion complex (Yılmaz and Yılmaz, 2004; Topuz and others, 2013a). The Kurtlutepe metamorphics include sub-greenschist-facies metavolcanic and volcanoclastic rocks (~65 % of the outcrop area), marble (~20 %), calc-phyllite (~15 %), and minor metachert and carbonated serpentinite. Marked differences in metamorphic-grade and tectonic position of the metamorphic domains in the Refahiye and Kurtlutepe areas indicate that the tectonic contacts in both domains are unrelated to each other (fig. 4B).

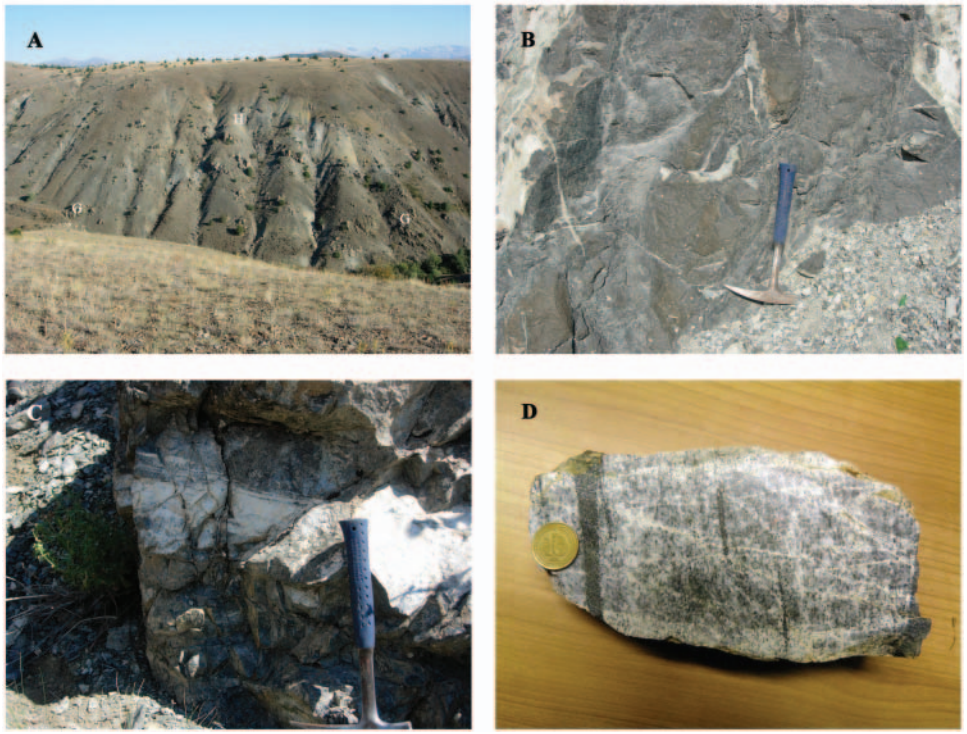

Fig. 5. Outcrop and hand-specimen pictures. (A) Gabbroic intrusions "G" within the serpentinized harzburgite "H", (B) slightly serpentinized massive harzburgite, (C) trondhjemite vein (light-colored) within the well-foliated gabbro, (D) polished surface of a trondhjemite sample (#343b) with pronounced igneous foliation.

ANALYTICAL TECHNIQUES

Whole-rock analyses were performed at Acme Analytical Laboratories Ltd. in Vancouver, Canada by ICP emission spectrography (Jarrel Ash AtomComb 975) for major elements and the trace elements Ba, Nb, Ni, Sr, Sc, Y and Zr, and an ICP mass spectrometer (Perkin-Elmer Elan 6000) for the determination of other trace elements including rare earth elements. Analytical procedures and levels of uncertainty are the same as outlined in Topuz and others (2010).

Major element compositions of the minerals were determined using the Jeol JXA-8900 RL wavelength dispersive electron microprobe (EMP) at the University of Mainz. Olivine, orthopyroxene, clinopyroxene, spinel and hornblende were analyzed using an accelerating potential of 20 kV, a beam current of 12 nA, and a spot size of 2 μm. Feldspars were analyzed with a defocused beam (10 μm) in order to minimize loss of alkalis. Natural and synthetic minerals were used for calibration.

Cathodo-luminescence images of the zircons were taken before in-situ LA-ICP-MS dating in the Geology Department of the Hacettepe University (Ankara) to characterize zircons to be dated. The CL images were produced by a Zeiss Evo-50 SEM equipped with cathode-luminescence and EDS detectors. LA-ICP-MS analyses for the zircons were performed at the Institute of Geosciences at Mainz, utilizing a system consisting of a New Wave 213 nm laser coupled to an Agilent 7500ce quadrupole ICP-MS. Analytical procedures are the same as outlined in Topuz and others (2010).

PETROGRAPHY AND MINERAL CHEMISTRY

Clinopyroxene-bearing harzburgite and dunite are massive to feebly foliated, and contain olivine, orthopyroxene, spinel and minor clinopyroxene (figs. 5B and 6A). Secondary phases are tremolite-hornblende, magnetite, serpentine, chlorite and talc. Clinopyroxene occurs either as inclusion in orthopyroxene, or forms individual grains. Feeble foliation is defined by the slightly parallel alignment of internally non-deformed orthopyroxene grains. The peridotites from the northwestern part of the study area (for example, sample # 444) display a marked tectonic fabric, defined by elongated olivine with deformation lamella, undulose extinction and bent orthopyroxene (fig. 6B), suggesting post-igneous deformation. Olivine (Fo_{90-92}) is homogeneous with NiO contents of 0.37 to 0.50 weight percent. Orthopyroxene shows clinopyroxene exsolution lamella, and the compositional range $Wo_{1-4}En_{86-94}Fs_{5-12}$ with variable Al_2O_3 and CaO contents, 1.06 to 4.85 and 0.30 to 2.19 weight percent, respectively (fig. 7A; table 1). Similarly, clinopyroxene ($Wo_{47-52}En_{45-53}Fs_{1-7}$) has variable Al_2O_3 contents of 1.26 to 4.60 weight percent (fig. 7B). Spinel displays $Mg/(Mg+Fe^{2+})$ and $Cr/(Cr+Al)$ of 0.38 to 0.76 and 0.18 to 0.62, respectively (fig. 7C; table 2). Only in the oxidized domains of spinel grains (sample #219), $Cr/(Cr+Al)$ values increase dramatically (0.62-0.89), associated with the decrease of $Mg/(Mg+Fe^{2+})$ values (0.40-0.25). With these compositional features, pyroxene and spinel resemble those from both the modern abyssal and depleted forearc peridotites (for example, Dick and Bullen, 1984; Hebert and others, 1990; Johnson and others, 1990; Ishii and others, 1990). Comparable compositional variations in spinel were also documented from the eastern part of the Refahiye ophiolite by Rice and others (2006) (dotted areas in fig. 7C). Pargasite inclusions are common in spinel. Late amphibole is represented by tremolite (table 3).

Clinopyroxenite contains totally serpentinized olivine grains up to 5 volume percent and minor Cr-Al spinel apart from the clinopyroxene. Clinopyroxene ($Wo_{45-50}En_{47-50}Fs_{3-5}$) is replaced by actinolite to hornblende along the fractures indicative of water ingress, and displays Al and Na contents of 0.009 to 0.080 and 0.001 to 0.013 cations per 3 oxygens, respectively (table 1). Dissimilar to Cr-Al spinel in the host peridotite, Cr-Al spinel has X_{Mg} values of 0.18 to 0.30 and $Cr/(Cr+Al)$ ratios of 0.48 to 0.61 (sample 96D in fig. 7C; table 2). Actinolite-hornblende displays variable Al_2O_3 (2.00-9.97 wt%), Cr_2O_3 (0.30-1.61 wt%) and Na_2O contents (0.31-1.67 wt%) (table 3).

Cumulate gabbro (*type-I*) is characterized by medium grain sizes (Ø~1-3 mm), and comprises clinopyroxene, plagioclase, and minor orthopyroxene and spinel (figs. 6C and 6D). Locally there are dark-colored strongly altered domains consisting of cumulus olivine (now serpentine), intercumulus cloudy-looking plagioclase and clinopyroxene. Overall the samples do not display any sign of deformation. Cloudy appearance in plagioclase is caused by alteration into a fine-grained intergrowth consisting of albite, pumpellyite and prehnite. Other secondary phases are serpentine, chlorite, calcite and actinolite.

Non-cumulate gabbro (*type-II*) is fine to medium-grained (~200 μm to 3 mm), and consist of plagioclase, hornblende, ilmenite, titanite and quartz, and accessory phases of apatite and zircon (figs. 6E and 6F). Absence of any anhydrous ferromagnesian minerals (olivine and pyroxene) is remarkable. Secondary phases are prehnite, pumpellyite, ±actinolite, ±chlorite, ±epidote, albite and ±K-feldspar. Gabbro displays feebly to well-developed foliation, defined by parallel alignment of hornblende and plagioclase, and concentration of ilmenite grains (a pseudocumulate texture). Both hornblende and plagioclase are mostly internally undeformed, suggesting a magmatic origin for the foliation (for example, Vernon, 2000). Hornblende has local inclusions of plagioclase, quartz and ilmenite, and displays Al_2O_3 and TiO_2 contents in the range 6.00 to 9.00 and 0.77 to 1.50 weight percent. Na_2O contents vary between

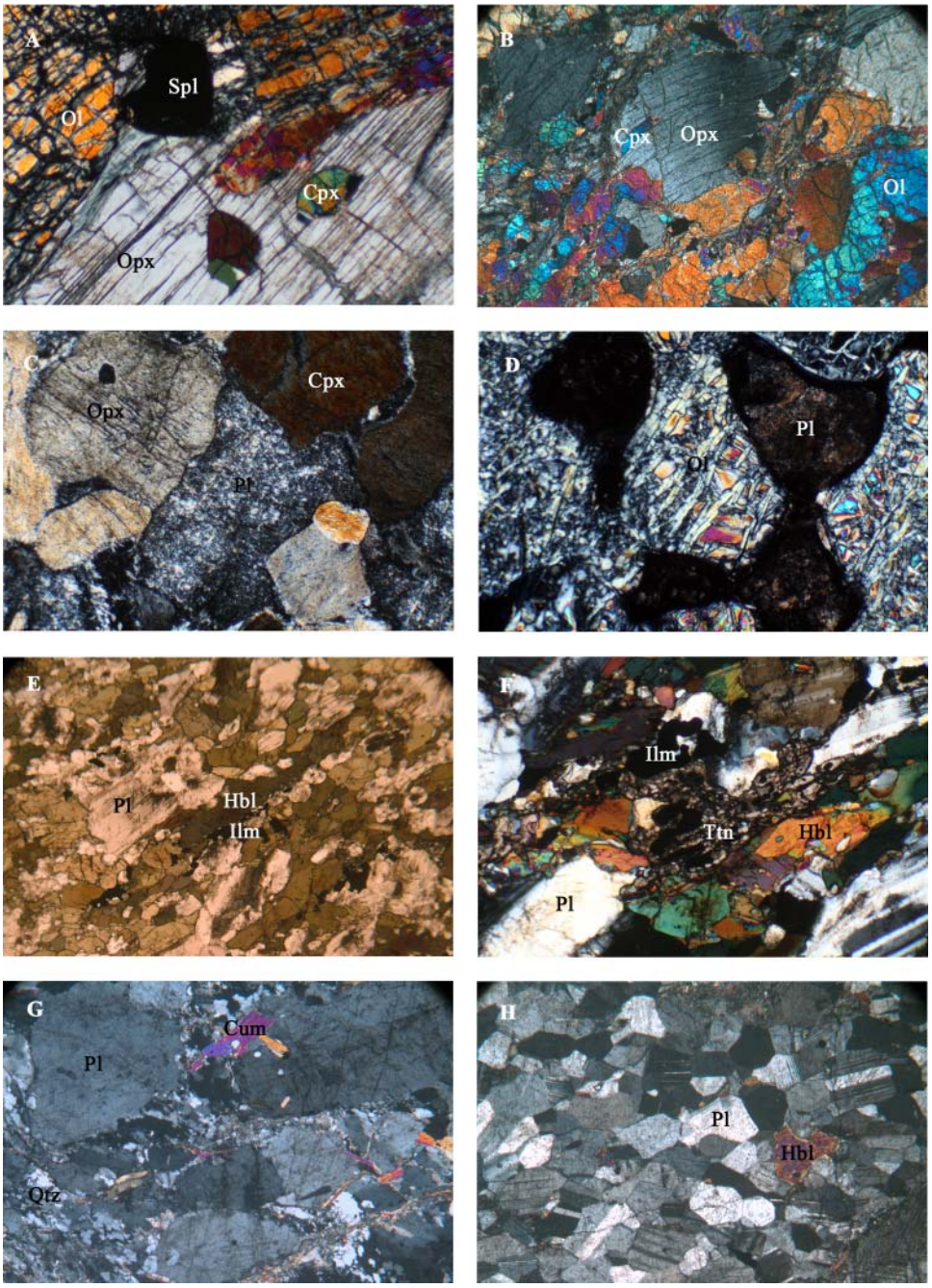

Fig. 6. Microtextural features of the different rock types in the Refahiye ophiolite. (A) Clinopyroxene occurs as inclusion in orthopyroxene (Cpx-bearing harzburgite #91). (B) Olivine with undulose extinction and bend orthopyroxene (harzburgite #442), (C) relic clino- and orthopyroxene in a cumulate gabbro. Cloudy-looking areas represent former plagioclase (cumulate gabbro #322), (D) cumulus olivine (partially serpentinized) and intercumulus plagioclase (totally altered) (cumulate gabbro #593e3). (E) Feebly elongated hornblende and plagioclase grains in gabbro. Note that the ilmenite grains are concentrated along the foliation plane. (non-cumulate gabbro #252) (F) Ilmenite is overgrown by titanite (non-cumulate gabbro #252). (G) Plagioclase grains in a dynamically recrystallized quartz matrix (trondhjemite, #605B). (H) A very plagioclase-rich trondhjemite (#342). The long side of the images is 4.4 mm.

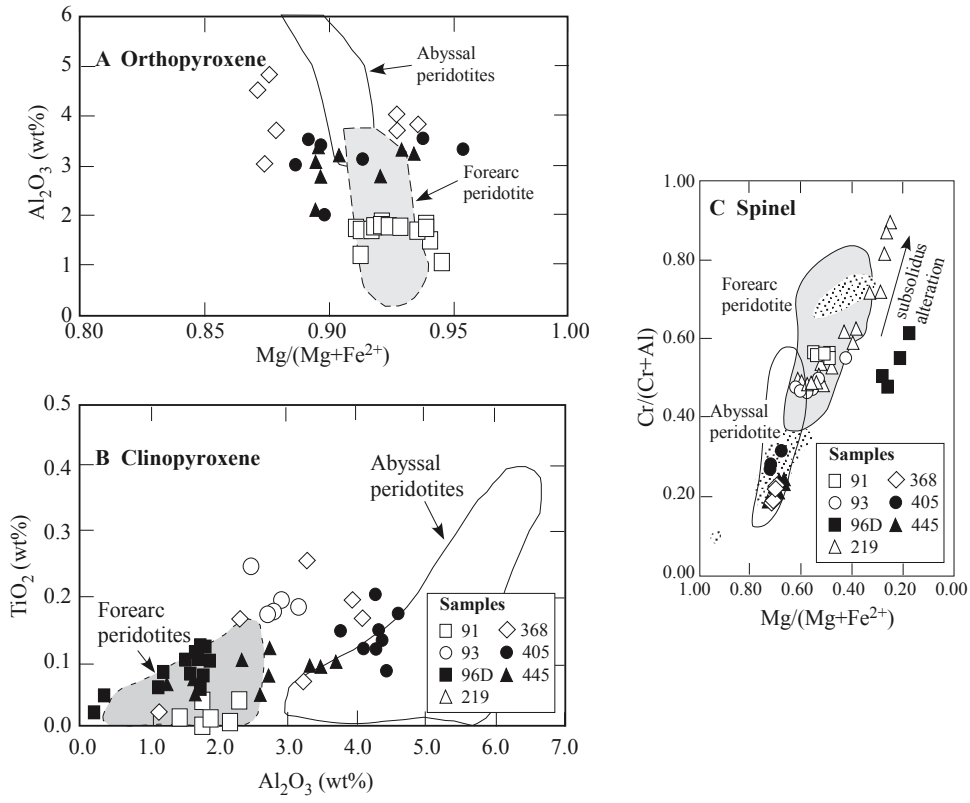

Fig. 7. Compositional variation of pyroxenes and spinels from the Refahiye peridotite (A) X_{Mg} vs Al_2O_3 contents in orthopyroxene. Fields for the abyssal and forearc peridotite are from Johnson and others (1990), and Ishii and others (1992), respectively. (B) TiO_2 vs. Al_2O_3 in clinopyroxene. Fields for abyssal and forearc peridotite are taken from Hebert and others (1990) and Ishii and others (1992), respectively. (C) X_{Mg} ($Mg/Fe^{2+}+Mg$) vs. X_{Cr} ($Cr/(Cr+Al)$) in spinel. Fields of abyssal and forearc peridotite are after Dick and Bullen (1984). Dotted areas represent the spinel compositions reported in Rice and others (2006).

0.90 to 1.50 weight percent (table 3). Plagioclase (An_{34-58}) is compositionally zoned with intrasample variation up to 35 mole percent, whereby the cores are characterized by An-richer compositions. Ilmenite has MnO contents up to 1.30 to 2.00 weight percent, and usually overgrown by titanite. Titanite is characterized by Al and Fe contents of 0.66 to 2.50 and 0.60 to 1.00 weight percent.

Trondhjemite displays a feeble foliation (fig. 5D), and comprises plagioclase, quartz, and subordinary cummingtonite, hornblende and biotite (figs. 6G and 6H). Accessory phases are apatite and zircon, and minor alteration minerals such as chlorite, prehnite, albite and actinolite are found. Cummingtonite is overgrown by hornblende. Modal composition varies considerably, from quartz-rich ones to quartz-poor ones. Interstitial quartz locally display dynamically recrystallized features (fig. 6G), suggesting that the deformation was also ongoing in subsolidus state. The cores of plagioclases (An_{27-36}) are characterized by An-richer compositions up to 6 mole percent. Cummingtonite is characterized by X_{Mg} values of 0.53 to 0.56, and Ca and Al contents of 0.13 to 0.198 and 0.175 to 0.280 cations per 23 oxygens (table 3). Hornblende is characterized, on the other hand, by Al_2O_3 and Na_2O contents of 5.62 to 10.08 weight percent, and 0.60 to 1.00 weight percent, respectively.

TABLE 1

Selected analyses of pyroxenes from the Refahiye peridotites, NE Turkey

Sample	91	91	93	93	368	368	405	405	445	91	91	368	368	405	405	444	444	96D
Rock type	HB	HB	DU	DU	HB	HB	HB	HB	HB	HB	HB	HB	HB	HB	HB	HB	HB	PX
Analyse	47	51	37	38	7	9	7	8	5	4	5	8	12	4	5	11	29	1
SiO_2	52.91	53.74	52.43	53.02	52.71	52.15	52.44	52.26	52.80	56.83	56.42	55.21	54.79	54.75	55.17	55.10	55.18	54.13
TiO_2	0.01	0.01	0.19	0.25	0.07	0.26	0.15	0.14	0.10	0.03	0.02	0.04	0.03	0.03	0.00	0.00	0.01	0.08
Al_2O_3	2.19	1.46	3.18	2.48	3.21	3.27	4.31	4.33	2.33	1.06	1.51	4.05	3.72	3.32	3.55	3.20	3.19	1.70
Cr_2O_3	0.96	0.51	1.19	0.75	0.68	0.90	1.54	1.45	0.50	0.98	0.39	0.61	0.62	0.78	0.98	0.53	0.60	0.66
FeO	2.26	2.06	2.08	2.15	1.86	2.07	1.91	1.95	1.85	5.70	6.23	6.48	6.63	5.53	5.42	6.28	6.31	3.34
MnO	0.13	0.03	0.05	0.07	0.00	0.07	0.07	0.09	0.07	0.14	0.16	0.13	0.18	0.12	0.17	0.17	0.18	0.12
NiO	n.a.	n.a.	0.09	0.05	0.04	0.09	0.04	0.02	0.03	0.09	0.13	0.10	0.11	0.09	0.10	0.10	0.09	n.a.
MgO	17.87	17.29	16.06	16.54	16.94	16.80	15.97	15.78	17.10	35.68	34.94	33.99	33.74	34.13	33.71	33.81	33.12	17.11
CaO	23.37	24.69	24.30	24.26	24.15	24.45	22.04	22.03	24.36	0.52	0.70	0.41	0.37	1.07	0.99	0.81	0.40	23.53
Na_2O	0.07	0.10	0.50	0.38	0.14	0.16	1.27	1.11	0.06	0.00	0.04	0.02	0.00	0.06	0.09	0.03	0.00	0.17
K_2O	0.01	0.00	0.00	0.00	0.01	0.00	0.01	0.01	0.00	0.00	0.02	0.00	0.00	0.01	0.01	0.02	0.00	0.00
Total	99.77	99.87	100.07	99.95	99.82	100.21	99.74	99.17	99.21	101.03	100.56	101.02	100.19	99.87	100.19	100.05	99.08	100.82
Normalized to six oxygens and four cations																		
Si	1.922	1.954	1.906	1.928	1.915	1.891	1.900	1.907	1.931	1.933	1.930	1.884	1.887	1.884	1.896	1.898	1.924	1.957
Ti	0.000	0.000	0.005	0.007	0.002	0.007	0.004	0.004	0.003	0.001	0.000	0.001	0.001	0.001	0.000	0.000	0.000	0.002
Al	0.094	0.062	0.136	0.106	0.137	0.140	0.184	0.186	0.100	0.043	0.061	0.163	0.151	0.135	0.144	0.130	0.131	0.072
Cr	0.027	0.015	0.034	0.021	0.019	0.026	0.044	0.042	0.015	0.026	0.010	0.016	0.017	0.021	0.027	0.014	0.016	0.019
Fe^{3+}	0.039	0.022	0.043	0.030	0.020	0.050	0.054	0.030	0.021	0.063	0.071	0.052	0.058	0.079	0.044	0.062	0.004	0.002
Fe^{2+}	0.029	0.041	0.020	0.036	0.037	0.013	0.004	0.029	0.035	0.099	0.107	0.133	0.133	0.080	0.111	0.119	0.180	0.098
Mn	0.004	0.001	0.002	0.002	0.000	0.002	0.002	0.003	0.002	0.004	0.005	0.004	0.005	0.003	0.005	0.005	0.005	0.004
Ni	0.000	0.000	0.003	0.001	0.001	0.003	0.001	0.000	0.001	0.003	0.004	0.003	0.003	0.002	0.003	0.003	0.003	-
Mg	0.968	0.937	0.870	0.897	0.917	0.908	0.862	0.858	0.932	1.809	1.782	1.729	1.732	1.751	1.727	1.736	1.721	0.922
Ca	0.910	0.962	0.946	0.945	0.940	0.950	0.855	0.861	0.955	0.019	0.026	0.015	0.014	0.039	0.036	0.030	0.015	0.912
Na	0.005	0.007	0.035	0.027	0.010	0.011	0.089	0.079	0.004	0.000	0.003	0.001	0.000	0.004	0.006	0.002	0.000	0.012
K	0.001	0.000	0.000	0.000	0.001	0.000	0.000	0.001	0.000	0.000	0.001	0.000	0.000	0.000	0.001	0.001	0.000	0.000
X_{Mg}	0.97	0.96	0.98	0.96	0.96	0.99	1.00	0.97	0.96	0.95	0.94	0.93	0.93	0.96	0.94	0.94	0.91	0.90
X_{En}	0.51	0.48	0.47	0.48	0.48	0.49	0.50	0.49	0.49	0.94	0.93	0.92	0.92	0.94	0.92	0.92	0.90	0.48
X_{Wol}	0.48	0.50	0.52	0.50	0.50	0.51	0.50	0.49	0.50	0.01	0.01	0.01	0.01	0.02	0.02	0.02	0.01	0.47
X_{Fs}	0.02	0.02	0.01	0.02	0.02	0.01	0.00	0.02	0.02	0.05	0.06	0.07	0.07	0.04	0.06	0.06	0.09	0.05

HB: Harzburgite, DU: Dunite; PX: Pyroxenite; $X_{Mg} = Mg/(Mg+Fe^{2+})$; $X_{En} = Mg/(Ca+Mg+Fe^{2+})$; $X_{Wol} = Ca/(Ca+Mg+Fe^{2+})$; $X_{Fs} = Fe^{2+}/(Ca+Mg+Fe^{2+})$, n.a. not analyzed.

TABLE 2

Selected analyses of Cr-Al spinels from the Refahiye ophiolite, NE Turkey

Sample	91	91	93	93	219	219	219	219	368	368	405	405	444	444	96D	96D
Comment	18	19	49	50	5	6	47	48	31	32	10	11	41	42	26	29
Rock Type	HB	HB	DU	DU	DU	DU	DU	DU	HB	HB	HB	HB	HB	HB	PX	PX
SiO_2	0.03	0.00	0.04	0.02	0.04	0.04	0.00	0.02	0.03	0.00	0.03	0.02	0.03	0.03	0.06	0.01
TiO_2	0.00	0.03	0.23	0.22	0.44	0.41	0.30	0.22	0.02	0.04	0.04	0.06	0.01	0.02	0.33	0.34
Al_2O_3	22.83	23.21	27.70	27.19	4.47	12.14	19.31	10.83	49.35	46.70	43.35	43.15	46.33	48.43	19.47	23.49
Cr_2O_3	44.58	44.28	37.75	38.05	55.13	45.20	41.14	40.71	18.33	20.36	25.08	25.64	21.43	19.10	35.67	35.28
FeO	20.54	20.64	20.64	21.07	33.66	33.36	29.92	40.02	13.74	14.70	13.48	13.35	14.10	14.45	36.16	33.06
MnO	0.21	0.09	0.19	0.10	0.44	0.29	0.36	0.50	0.10	0.11	0.20	0.15	0.15	0.13	0.39	0.38
NiO	0.07	0.11	0.16	0.14	0.14	0.15	0.10	0.13	0.29	0.26	0.20	0.16	0.21	0.24	n.a.	n.a.
MgO	11.97	11.83	13.71	13.03	4.68	6.56	8.28	5.64	17.01	16.69	17.41	17.32	16.64	16.69	4.17	5.84
CaO	0.00	0.00	0.00	0.00	0.00	0.00	0.00	0.09	0.00	0.00	0.00	0.09	0.01	0.02	0.48	0.18
Na_2O	0.02	0.02	0.00	0.01	0.02	0.00	0.01	0.00	0.03	0.01	0.00	0.00	0.00	0.03	0.04	0.03
K_2O	0.01	0.00	0.00	0.01	0.00	0.00	0.01	0.00	0.00	0.00	0.01	0.00	0.00	0.00	0.01	0.01
Total	100.25	100.22	100.41	99.82	99.02	98.14	99.43	98.15	98.89	98.87	99.80	99.94	98.90	99.14	96.78	98.61
Cations per 4 oxygens and 3 cations																
Si	0.001	0.000	0.001	0.001	0.001	0.001	0.000	0.001	0.001	0.000	0.001	0.000	0.001	0.001	0.002	0.000
Ti	0.000	0.001	0.005	0.005	0.012	0.010	0.007	0.006	0.000	0.001	0.001	0.001	0.000	0.000	0.008	0.008
Al	0.828	0.842	0.973	0.965	0.186	0.485	0.732	0.437	1.587	1.520	1.412	1.406	1.510	1.563	0.775	0.895
Cr	1.085	1.077	0.889	0.906	1.541	1.212	1.046	1.102	0.396	0.444	0.548	0.560	0.469	0.413	0.952	0.902
Fe^{3+}	0.083	0.075	0.122	0.113	0.245	0.276	0.201	0.443	0.016	0.035	0.037	0.030	0.020	0.023	0.255	0.188
Fe^{2+}	0.446	0.456	0.392	0.418	0.750	0.670	0.603	0.702	0.298	0.304	0.275	0.278	0.307	0.308	0.766	0.706
Mn	0.006	0.002	0.005	0.003	0.013	0.008	0.010	0.014	0.002	0.002	0.005	0.003	0.004	0.003	0.011	0.010
Ni	0.002	0.003	0.004	0.003	0.004	0.004	0.003	0.003	0.006	0.006	0.004	0.004	0.005	0.005	0.000	0.000
Mg	0.549	0.543	0.609	0.585	0.247	0.332	0.397	0.288	0.692	0.687	0.717	0.714	0.686	0.681	0.210	0.281
Ca	0.000	0.000	0.000	0.000	0.000	0.000	0.000	0.003	0.000	0.000	0.000	0.003	0.000	0.000	0.017	0.006
Na	0.001	0.001	0.000	0.000	0.001	0.000	0.000	0.000	0.001	0.001	0.000	0.000	0.000	0.002	0.003	0.002
K	0.000	0.000	0.000	0.000	0.000	0.000	0.000	0.000	0.000	0.000	0.000	0.000	0.000	0.000	0.000	0.000
Total	3.000	3.000	3.000	3.000	3.000	3.000	3.000	3.000	3.000	3.000	3.000	3.000	3.000	3.000	3.000	3.000
X_{Mg}	0.55	0.54	0.61	0.58	0.25	0.33	0.40	0.29	0.70	0.69	0.72	0.72	0.69	0.69	0.22	0.29
X_{Cr}	0.57	0.56	0.48	0.48	0.89	0.71	0.59	0.72	0.20	0.23	0.28	0.29	0.24	0.21	0.55	0.50

HB: Harzburgite; DU: Dunite; PX: Pyroxenite; $X_{Mg} = Mg/(Mg+Fe^{2+})$; $X_{Cr} = Cr/(Cr+Al)$.

TABLE 3

Selected analyses of amphibole from Refahiye ophiolite, NE Turkey

Sample	96B	96B	252	252	270	270	272	272	96A	96A	96A	96A	96D	96D	93	93	93
Analyse	2	9	1	2	4	27	47	54	1	2	9	42	8	9	48	50	4
Type	MgHbl	MgHbl	MgHbl	MgHbl	MgHbl	MgHbl	MgHbl	MgHbl	Cum	Cum	MgHbl	Act	Tre	MgHbl	Tre	Tre	Parg
Rock Type	GB	GB	GB	GB	GB	GB	GB	GB	TR	TR	TR	TR	PX	PX	HB	HB	DU
SiO_2	46.36	45.40	45.59	45.81	46.09	46.79	44.38	44.18	52.85	53.07	45.24	53.499	54.45	48.26	56.72	57.05	41.71
TiO_2	1.20	1.05	1.15	1.13	0.94	0.84	1.06	0.58	0.16	0.04	0.08	0.14	0.15	0.48	0.01	0.00	0.51
Al_2O_3	7.10	8.34	8.25	7.90	8.21	7.08	9.45	9.52	1.61	1.00	10.08	1.546	3.78	9.27	1.81	1.29	14.62
Cr_2O_3	0.08	0.00	0.01	0.07	0.00	0.06	0.00	0.00	0.03	0.01	0.00	0.023	0.61	1.24	0.49	0.34	2.74
FeO	18.35	17.92	19.46	18.84	18.35	17.36	20.39	20.14	25.03	24.87	18.37	15.12	3.80	4.82	2.08	2.82	3.67
MnO	0.43	0.20	0.34	0.40	0.28	0.29	0.33	0.28	0.58	0.75	0.32	0.399	0.09	0.11	0.13	0.01	0.00
MgO	10.78	10.53	10.03	10.21	10.41	11.43	9.00	8.63	15.85	16.14	10.75	14.579	21.43	18.96	23.26	23.03	17.99
CaO	11.28	11.69	11.31	11.40	11.69	11.76	11.42	11.50	1.25	0.88	10.56	12.113	12.54	12.46	12.81	13.08	12.87
Na_2O	1.12	1.08	1.23	1.16	0.98	0.76	1.19	1.11	0.15	0.21	0.86	0.124	0.70	1.65	0.14	0.06	3.65
K_2O	0.27	0.30	0.30	0.29	0.28	0.23	0.33	0.43	0.01	0.00	0.20	0.033	0.01	0.01	0.02	0.04	0.06
Total	96.96	96.52	97.66	97.20	97.23	96.60	97.55	96.37	97.52	96.96	96.46	97.58	97.55	97.24	97.47	97.72	97.82
Based on 23 oxygens and average Fe^{+3} calculation after Schumacher (1997)																	
Si	6.938	6.822	6.805	6.861	6.874	6.973	6.666	6.725	7.815	7.889	6.720	7.772	7.517	6.783	7.760	7.807	5.938
$Al^{[4]}$	1.062	1.178	1.195	1.139	1.126	1.027	1.334	1.275	0.185	0.111	1.280	0.228	0.483	1.217	0.240	0.193	2.062
$Al^{[6]}$	0.190	0.299	0.256	0.255	0.317	0.216	0.338	0.433	0.096	0.064	0.485	0.036	0.131	0.319	0.052	0.016	0.391
Ti	0.135	0.119	0.129	0.127	0.106	0.095	0.120	0.067	0.018	0.005	0.009	0.015	0.015	0.051	0.001	0.000	0.054
Fe^{+3}	0.419	0.394	0.471	0.412	0.403	0.483	0.521	0.430	0.047	0.037	0.739	0.153	0.212	0.342	0.129	0.133	0.294
Cr	0.009	0.000	0.002	0.008	0.000	0.007	0.000	0.000	0.004	0.001	0.000	0.003	0.067	0.138	0.053	0.037	0.308
Mg	2.405	2.359	2.231	2.279	2.315	2.540	2.014	1.959	3.495	3.575	2.380	3.157	4.410	3.972	4.745	4.699	3.818
Fe^{+2}	1.877	1.857	1.959	1.949	1.887	1.680	2.041	2.134	3.049	3.054	1.543	1.684	0.226	0.223	0.108	0.189	0.143
Mn	0.054	0.026	0.043	0.050	0.035	0.037	0.042	0.036	0.072	0.094	0.041	0.049	0.010	0.013	0.015	0.001	0.000
Ca_B	1.809	1.882	1.809	1.829	1.867	1.877	1.838	1.875	0.199	0.141	1.681	1.885	1.854	1.876	1.878	1.917	1.963
Na_B	0.102	0.063	0.102	0.091	0.071	0.066	0.086	0.067	0.022	0.029	0.123	0.017	0.073	0.066	0.018	0.008	0.029
Na_A	0.224	0.252	0.255	0.246	0.213	0.154	0.259	0.262	0.022	0.030	0.125	0.017	0.113	0.382	0.018	0.008	0.979
K_A	0.052	0.057	0.056	0.055	0.053	0.044	0.063	0.083	0.003	0.000	0.038	0.006	0.002	0.001	0.004	0.007	0.010
X_{Mg}	0.56	0.56	0.53	0.54	0.55	0.60	0.50	0.48	0.53	0.54	0.61	0.65	0.95	0.95	0.98	0.96	0.96

Amphibole Types: MgHbl: Magnesiohornblende; Cum: Cummingtonite; Act: Actinolite; Tre: Tremolite; Parg: Pargasite (inclusion in spinel); Rock types: GB: Non-cumulate gabbro; TR: Trondhjemite; PX: Pyroxenite; HB: Harzburgite; DU: Dunite.

BULK-ROCK CHEMISTRY

Representative whole-rock analyses of the cumulate gabbro (type-1), noncumulate gabbro (type-2), pegmatitic gabbro and trondhjemite are given in table 4. As indicated above, the samples are variably overprinted by the subgreenschist-facies hydrothermal metamorphism. Samples with minimal hydrothermal overprint were selected for analysis. Loss on ignition values range from 3.60 to 5.00 weight percent in the cumulate gabbro, from 0.70 to 1.80 weight percent in noncumulate gabbros, and 0.40 to 3.80 in trondhjemites. These values are related to the relative amounts of the igneous hydrous phases (amphibole, ±biotite) together with the hydrothermal ones (prehnite, pumpellyite, chlorite, actinolite and epidote). In the petrological considerations we rely only on the relative abundances in the high-field strength and rare earth elements which are mostly regarded as immobile during the low-grade metamorphism (for example, Rollinson, 1995).

Cumulate gabbro (*type-I*) has low SiO_2 (43-46 wt%), high Al_2O_3 (16-18 wt%) and high MgO contents (12-13 wt%) (table 4). Mg numbers [Mg# = molecular MgO/(MgO+FeO*)] are anomalously high, ranging from 0.85 to 0.88. REE patterns are slightly fractionated ($(La/Yb)_{cn}$ ~1.19) and display significant positive Eu anomalies (Eu/Eu* ~1.61-1.84) (fig. 8A). All these geochemical features are in line with the cumulate nature.

Non-cumulate gabbro (*type-II*) is characterized by narrow compositional range SiO_2 (45-52 wt%), TiO_2 (1.26-2.11 wt%), Al_2O_3 (14-16 wt%) and K_2O (0.08-0.67 wt%). Mg numbers range from 0.39 to 0.53. The Cr and Ni contents are low (Cr ≤ 144 ppm, Ni ~4-28 ppm). Despite the presence of locally well-developed igneous foliation, bulk-rock compositions do not show any indication for a cumulate nature. The gabbro displays nearly flat REE patterns with $(La/Yb)_{cn}$ and insignificant Eu/Eu* values of 0.51 to 1.07 and 0.86 to 1.04, respectively (fig. 8B). On the multi-element variation diagrams the gabbros have slightly negative Nb-Ta through, and K, Pb and Sr anomalies ranging from positive to negative with respect to MORB composition, which is probably related to the subsolidus hydrothermal metamorphism (fig. 9B). With all these geochemical features, the gabbro resemble arc tholeiites.

Trondhjemite, used here as a general term to refer to felsic quartzo-feldspathic dikes, displays highly variable SiO_2 (51-76 wt%), Al_2O_3 (13-27 wt%) and CaO (3-12 wt%) contents, reflecting variable modal amounts of quartz and plagioclase. In clear distinction to the host type-2 gabbro, the trondhjemite displays variably fractionated concave upward REE patterns with $(La/Yb)_{cn}$~3–23, and pronounced positive Eu anomaly (Eu/Eu*~1.72-10.47; fig. 8C). On the multi element variation diagrams (fig. 9C), the trondhjemite displays highly variable intersample patterns with positive anomalies of Sr, Eu, Pb and Zr-Hf with respect to MORB composition. Several microstructural and geochemical features, for example (i) high concentration and parallel alignment of plagioclases (see Vernon and Collins, 2011), (ii) highly variable plagioclase-controlled bulk-rock chemical and modal composition (for example, strong variations in SiO_2, Al_2O_3 and CaO contents), and (iii) marked positive Eu anomaly imply a "cumulate flavor." However, we regard the cumulative processes as highly unlikely to have occurred in ≤50 cm-thick veins. There are two possibilities: (i) a melt phase was expelled from the veins after the crystallization of plagioclase due to differential stress, or (ii) trondhjemite was emplaced as a "plagioclase+melt mush."

GEOCHRONOLOGY

To constrain timing of the ophiolite formation, we carried out *in-situ* LA-ICP-MS U-Pb dating on zircons from two trondhjemite samples (96A and 746C; fig. 3). The sample 746C is from the easternmost part of the Refahiye ophiolite to the east of the NAF outside the study area. Both samples are feebly foliated, and consist of plagioclase,

TABLE 4

Whole-rock analyses of selected samples from the intrusive rocks in the Refahiye ophiolite, NE Turkey

Sample	317C	322	96B	252	270	272	343A	358A	618	634B	358B
Rock type	CG	CG	GAB	GAB	GAB	GAB	GAB	GAB	GAB	GAB	GAB
SiO_2	45.59	43.40	50.74	51.58	49.77	51.73	48.04	49.63	46.03	44.93	50.89
TiO_2	0.08	0.07	1.65	1.55	1.26	1.59	1.87	1.96	1.63	2.11	2.03
Al_2O_3	16.26	17.99	15.11	14.88	15.77	16.48	15.19	15.1	14.49	14.65	13.87
Fe_2O_3	4.35	3.68	12.09	12.40	11.01	11.55	15.13	13.41	14.74	14.85	13.81
MnO	0.09	0.07	0.20	0.20	0.18	0.18	0.23	0.19	0.23	0.22	0.21
MgO	12.05	13.24	5.56	5.46	6.15	4.47	5.37	4.45	7.58	7.39	4.40
CaO	16.28	14.68	8.90	9.53	9.95	8.50	9.06	9.06	11.64	10.76	8.55
Na_2O	1.32	1.23	3.92	3.14	3.18	3.83	3.87	4.20	2.48	3.01	4.54
K_2O	0.06	0.06	0.54	0.26	0.58	0.67	0.18	0.31	0.08	0.13	0.21
P_2O_5	0.01	0.01	0.16	0.13	0.11	0.14	0.16	0.12	0.16	0.18	0.17
LOI	3.60	5.00	0.90	0.70	1.80	0.70	0.70	1.20	0.70	1.50	1.10
Total	99.76	99.72	99.80	99.82	99.8	99.83	99.79	99.63	99.77	99.75	99.82
Sc	43	24	35	37	38	31	42	42	50	43	36
Ni	126.9	245.3	24.7	28.3	23.6	13.3	8.3	4.3	20.2	20.3	8.6
Cr	5713	1970	144	41	109	21	<14	<14	109	96	21
Co	37.6	36.3	34.4	33.1	33.7	30.6	42.4	40.5	46.9	45.7	34.4
V	112	64	313	366	326	343	519	541	447	491	433
Cu	156	108.6	54.4	22.8	46.0	39.8	96.9	1393.8	99.8	137.5	66.2
Zn	7	6	23	16	9	19	30	26	23	23	22
Ga	8.6	8.0	18.4	17.8	17.5	19.2	17.6	17.1	16.8	17.4	17.8
Cs	<0.1	0.5	<0.1	<0.1	<0.1	<0.1	0.2	<0.1	0.1	3.6	<0.1
Rb	0.7	2.0	7.5	2.2	7.0	8.6	2.3	2.8	0.6	1.9	1.6
Ba	10	44	106	54	73	80	48	101	19	55	43
U	<0.1	<0.1	0.2	<0.1	<0.1	0.2	<0.1	0.1	<0.1	<0.1	0.2
Th	<0.2	<0.2	0.6	0.6	0.5	0.8	<0.2	0.2	<0.2	<0.2	0.5
Pb	<0.1	0.1	0.6	0.3	0.4	0.3	0.3	1.1	0.2	0.2	0.5
Sr	106.4	439	234.3	143.1	226.7	220.4	206	308.7	127.8	196.3	170.1
Nb	0.4	<0.1	2.7	2.2	2.0	2.2	2.3	2.0	2.2	2.9	3.0
Ta	<0.1	<0.1	0.2	0.1	0.1	0.2	0.2	0.1	0.2	0.2	0.2
Zr	5.1	1.3	118.2	107	78.4	96.5	87.7	80.3	66.3	106.4	116.2
Hf	<0.1	<0.1	3.1	3.1	2.2	2.8	2.5	2.4	2.3	2.7	3.4
Y	2.3	1.8	37.6	34.4	28.3	33.8	37.9	29.5	44.2	38.2	40.9
La	0.3	<0.1	5.6	5.6	4.2	4.6	4.0	3.9	3.3	4.6	5.5
Ce	0.8	0.2	15.6	14.6	11.6	13.2	12.3	10.4	12.3	13.7	16.4
Pr	0.09	<0.02	2.43	2.26	1.83	2.00	2.09	1.67	2.19	2.22	2.48
Nd	0.5	<0.3	12.5	11.2	9.4	11.1	10.7	8.6	13.3	12.1	13.4
Sm	0.18	0.11	3.88	3.44	2.82	3.42	3.7	2.92	4.22	3.84	4.28
Eu	0.12	0.10	1.36	1.26	1.06	1.23	1.31	1.20	1.45	1.29	1.50
Gd	0.29	0.25	5.13	4.88	3.94	4.61	5.38	4.24	6.25	5.48	6.17
Tb	0.06	0.05	1.02	0.95	0.77	0.89	0.99	0.79	1.15	1.02	1.14
Dy	0.37	0.33	6.00	5.79	4.43	5.4	6.58	4.98	7.24	6.42	7.00
Ho	0.09	0.06	1.34	1.22	0.97	1.20	1.36	1.10	1.57	1.39	1.57
Er	0.23	0.17	4.15	3.66	3.17	3.6	4.05	3.21	4.56	4.12	4.72
Tm	0.03	0.02	0.60	0.57	0.47	0.54	0.62	0.51	0.70	0.61	0.70
Yb	0.17	0.15	3.88	3.52	2.85	3.63	3.94	3.12	4.33	3.84	4.44
Lu	0.03	0.02	0.59	0.54	0.43	0.52	0.59	0.48	0.65	0.58	0.68
Mg#	0.85	0.88	0.48	0.47	0.53	0.43	0.41	0.40	0.50	0.50	0.39
$(La/Yb)_{cn}$	1.19	-	0.97	1.07	0.99	0.85	0.68	0.84	0.51	0.81	0.84
$(La/Gd)_{cn}$	0.86	-	0.91	0.96	0.89	0.83	0.62	0.77	0.44	0.70	0.74
$(Gd/Yb)_{cn}$	1.56	1.47	1.16	1.19	1.19	1.08	1.11	1.12	1.17	1.17	1.13
Eu/Eu*	1.61	1.84	0.93	0.94	0.97	0.95	0.90	1.04	0.86	0.86	0.89

TABLE 4
(continued)

Sample	605C	348B	350	358E	96A	342	343B	605B	636C	
Rock type	GAB	PG	PG	PG	TR	TR	TR	TR	TR	MDL
SiO_2	49.18	45.34	45.31	53.97	75.61	54.83	51.19	74.35	54.39	0.01
TiO_2	1.68	0.13	0.63	0.27	0.10	0.17	0.26	0.28	0.20	0.01
Al_2O_3	14.13	22.73	18.77	19.27	14.13	26.54	23.86	13.00	21.37	0.01
Fe_2O_3*	12.99	4.17	6.34	3.11	0.93	1.00	2.14	1.94	1.57	0.04
MnO	0.21	0.08	0.12	0.09	0.02	0.02	0.03	0.04	0.04	0.01
MgO	5.44	8.04	10.10	5.82	0.54	0.55	1.53	0.78	2.44	0.01
CaO	10.89	15.17	14.57	9.93	3.49	9.71	11.69	3.49	10.79	0.01
Na_2O	3.47	1.19	1.30	4.92	4.54	6.05	5.39	5.55	5.73	0.01
K_2O	0.32	0.12	0.13	0.11	0.10	0.13	0.06	0.12	0.14	0.01
P_2O_5	0.11	<0.01	<0.01	0.07	0.02	<0.01	0.05	0.03	0.05	0.01
LOI	1.40	2.80	2.30	2.30	0.50	1.00	3.80	0.40	3.20	-5.10
Total	99.81	99.82	99.72	99.85	99.99	99.96	99.95	99.98	99.90	
Sc	40	23	29	13	2	2	3	2	3	1
Ni	18.3	4.0	59.1	10.6	25.9	3.7	4.9	2.2	6.1	0.1
Cr	55	<14	582	89	<14	<14	<14	<14	<14	14
Co	38.3	31.9	33.3	15.2	2.6	3.0	6.2	3.8	5.0	0.2
V	449	86	247	92	24	26	51	20	<8	8
Cu	74.8	1.9	3.1	2.1	3.4	0.4	2.6	5.9	1.2	0.1
Zn	19	6	4	2	4	4	6	12	12	1
Ga	17.2	14.1	14.9	13.8	11.7	20.5	18.6	12.2	14.5	0.5
Cs	0.1	<0.1	<0.1	<0.1	<0.1	<0.1	0.2	<0.1	0.1	0.1
Rb	2.3	1.3	0.9	0.9	0.8	1.2	1.7	0.6	1.7	0.1
Ba	62	61	55	98	124	27	27	96	126	1
U	0.1	<0.1	<0.1	0.1	0.9	<0.1	<0.1	0.3	2.0	0.1
Th	0.2	<0.2	<0.2	0.6	1.4	<0.2	<0.2	5.3	16.1	0.2
Pb	0.3	0.6	1.1	1.1	1.6	0.4	0.3	0.5	29.9	0.1
Sr	200.8	571.0	758.3	478.5	190.1	387.3	313.5	153.6	448.1	0.5
Nb	1.3	0.3	6.7	2.8	1.8	0.3	0.5	1.9	11.2	0.1
Ta	0.1	<0.1	0.4	0.1	<0.1	<0.1	<0.1	<0.1	0.5	0.1
Zr	72.3	5.3	29.8	93.7	127.7	145.9	73.2	144.6	119.7	0.1
Hf	2.3	0.2	1.4	2.3	3.4	3.1	1.9	4.2	3.5	0.1
Y	30.5	3.7	20.9	11.7	2.5	2.5	4.1	4.1	8.0	0.1
La	3.1	1.5	6.1	7.6	4.9	1.5	1.7	23.8	33.8	0.1
Ce	9.4	2.6	16.4	14.9	6.8	2.1	3.1	38.5	65.8	0.1
Pr	1.52	0.36	2.32	1.63	0.64	0.23	0.40	3.62	6.09	0.02
Nd	8.7	1.5	11.2	6.3	1.6	1.0	1.6	11.1	20.3	0.3
Sm	2.92	0.42	2.68	1.53	0.23	0.22	0.41	1.37	3.21	0.05
Eu	1.15	0.34	0.96	0.64	0.63	0.77	0.78	0.61	1.57	0.02
Gd	4.47	0.51	3.32	1.80	0.22	0.23	0.51	0.86	2.22	0.05
Tb	0.83	0.10	0.57	0.31	0.07	0.05	0.10	0.12	0.29	0.01
Dy	5.38	0.62	3.45	1.97	0.28	0.34	0.56	0.66	1.47	0.05
Ho	1.19	0.12	0.73	0.40	0.10	0.08	0.14	0.12	0.28	0.02
Er	3.49	0.40	2.11	1.23	0.32	0.29	0.42	0.48	0.85	0.03
Tm	0.53	0.06	0.31	0.20	0.08	0.05	0.08	0.08	0.15	0.01
Yb	3.29	0.39	1.94	1.28	0.44	0.39	0.53	0.69	1.13	0.05
Lu	0.51	0.06	0.28	0.21	0.12	0.08	0.10	0.14	0.23	0.01
Mg#	0.45	0.79	0.76	0.79	0.53	0.52	0.59	0.44	0.75	
$(La/Yb)_{cn}$	0.64	2.59	2.12	4.00	7.51	2.59	2.16	23.25	20.17	
$(La/Gd)_{cn}$	0.58	2.46	1.54	3.53	18.61	5.45	2.78	23.12	12.72	
$(Gd/Yb)_{cn}$	1.11	1.13	1.30	1.07	0.70	0.57	0.83	0.77	1.13	
Eu/Eu*	0.97	2.25	0.98	1.18	8.56	10.47	5.22	1.72	1.80	

CG: Cumulate gabbro (Type-I); GAB = Gabbro (Type-II); PG: Pegmatitic gabbro; TR: Trondhjemite; Mg# = $(MgO/(MgO+FeO_{tot}))$ in molar proportions; $_{cn}$ = chondrite-normalized; $Eu/Eu^* = Eu_{cn}/(Sm_{cn} \cdot Gd_{cn})^{0.5}$; oxides are given in wt%. trace elements in μg/g. MDL detection limits.

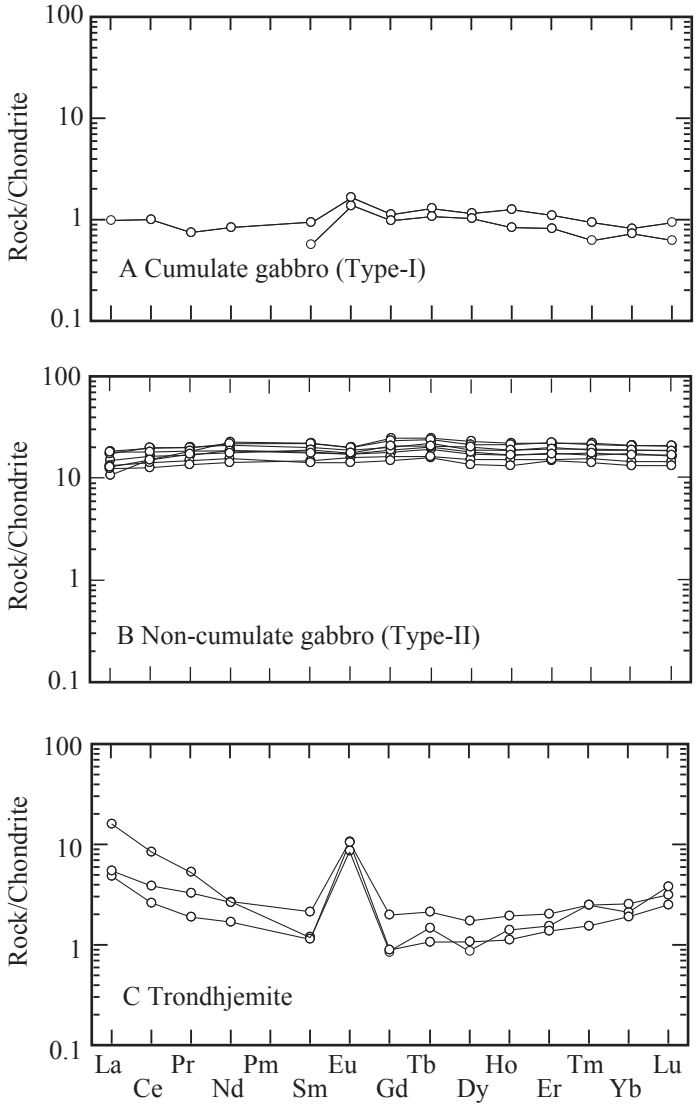

Fig. 8. Chondrite-normalized rare earth element patterns. Normalizing values were taken from Boynton (1984).

quartz and minor hornblende, ± cummingtonite and biotite. Apatite and zircon are accessory phases.

Zircons are mostly euhedral, and display oscillatory and sector zoning (fig. 10). However it contains local irregular domains indicative of recrystallization. High U contents (443-1960 ppm) and relatively high Th/U ratios (0.11-1.08) and oscillatory zoning are characteristic of the zircons grown from a melt phase (table 5; Hoskin and Schaltegger, 2003). 11 and 13 grains of zircon from sample 96A and 746 were analyzed for their U-Pb isotopic compositions, yielding concordia ages of 186 ± 4 Ma and 178 ± 4 Ma (2σ), respectively (fig. 11). In general, there is a large spread of the U-Pb isotopic data especially in sample 96A that cannot be accounted for by a single zircon

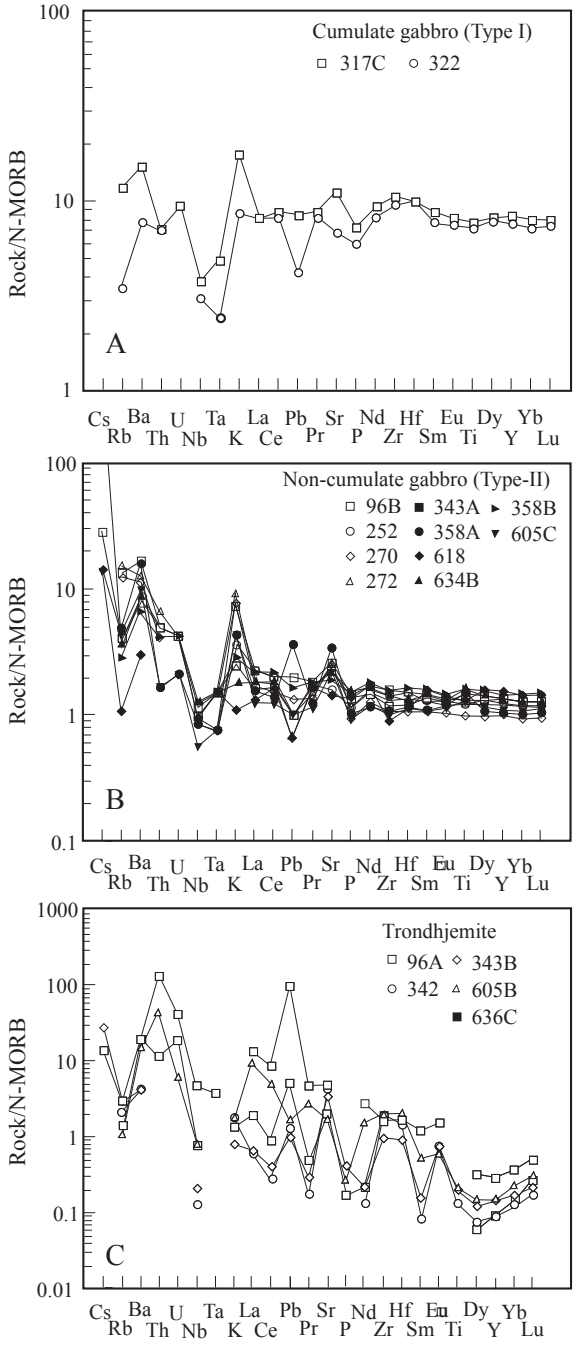

Fig. 9. N-MORB-normalized trace element abundance patterns (normalized to values given in Sun and McDonough, 1989).

population. Furthermore, there is a rough correlation between Th/U ratios of the dated zircons and the obtained age values (not shown).

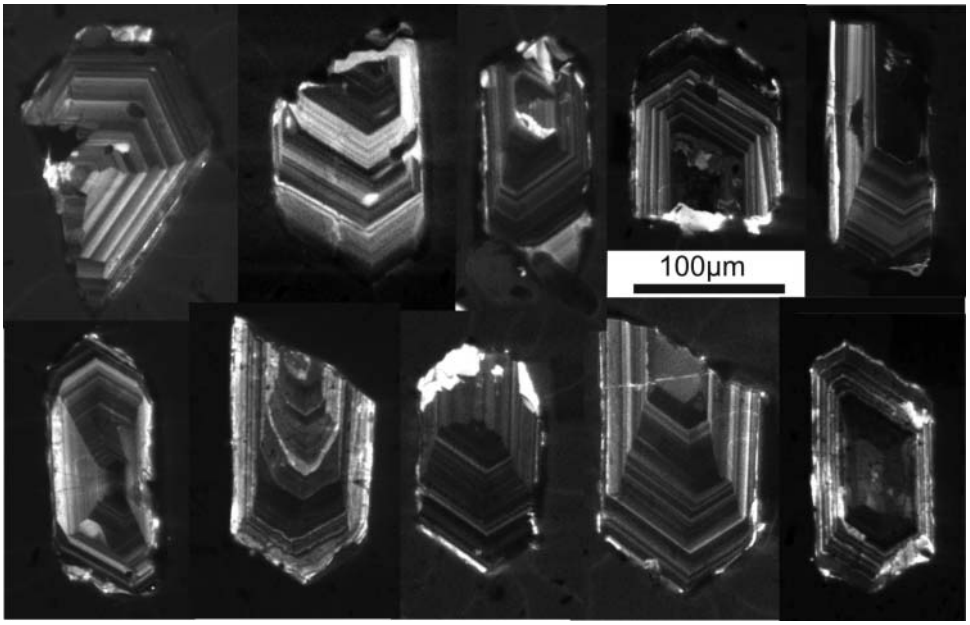

Fig. 10. Cathodoluminescence (CL) images of the dated zircons (sample # 746C).

Zircons have high U-Pb isotopic closure temperature (for example, Lee and others, 1997; Cherniak and Watson, 2000). On the basis of the topological and geochemical features of the analyzed grains, the U-Pb zircon date of 186 ± 4 Ma and 178 ± 4 Ma (2σ; Pliensbachien to Toarcien, Ogg and others, 2008) are regarded as the age of magmatic crystallization, while the recrystallization occurred shortly after the formation within the analytical uncertainty of the geochronological data, and accordingly approximates the time of the oceanic spreading. These zircon ages are slightly older than the two Ar-Ar plateau ages of the hornblende from the associated foliated gabbros (sample 96B: 174 ± 4 Ma, 2σ; sample 252: 173 ± 4 Ma, 2σ; see fig. 4A), which are interpreted as cooling ages below 500 to 580 °C of the gabbroic rocks (Topuz and others, 2013a). All these age values consistently suggest that the Refahiye ophiolite formed during early Jurassic time.

DISCUSSION

Arc tholeiitic affinity of the locally foliated non-cumulate gabbros indicate formation in a suprasubduction-zone environment (for example, Miyashiro, 1973; Pearce and others, 1984), as suggested by Rice and others (2006, 2009), Sarıfakıoğlu and others (2009) and Parlak and others (2013) on the basis of bulk rock geochemistry on basic rocks and spinel composition from the mantle rocks from the eastern end of the Refahiye ophiolite. The mantle peridotite contains low to high Cr# spinels together with low- to high-Al pyroxenes dependent on the location, encompassing the compositional fields defined by modern forearc and partly abyssal peridotites (fig. 7). This geochemical duality/transition is documented in most suprasubduction-zone ophiolites (for example, Choi and others, 2008; Rollinson, 2008; Uysal and others, 2009), and can be explained either by (i) transformation of former MORB-type (abyssal) domain to a suprasubduction one because of a fracture zone becoming a juvenile subduction zone due to rotation pole shift (Casey and Dewey, 1984; Dewey and Casey,

TABLE 5

LA-ICP-MS U-Th-Pb isotopic data and calculated ages for zircon grains from the trondhjemite, Refahiye Ophiolite, NE Turkey

Analysis	U	Th	Th/U	$^{208}Pb/^{232}Th$	$^{207}Pb/^{235}U$	$^{206}Pb/^{238}U$	rho	$^{207}Pb/^{206}Pb$	$^{208}Pb/^{232}Th$ Age (Ma)	$^{207}Pb/^{235}U$ Age (Ma)	$^{206}Pb/^{238}U$ Age (Ma)
Sample 96A											
1#*	1005	658	0.65	0.0152(12)	0.406(32)	0.0307(17)	0.45	0.0958(71)	305±23	346±24	195±11
2#*	446	166	0.37	0.0087(03)	0.181(08)	0.0271(06)	0.45	0.0485(19)	1760±6	169±7	1721±4
3#	1465	1222	0.83	0.0091(02)	0.214(07)	0.0311(07)	0.61	0.0498(14)	183±4	197±6	198±5
4#	805	214	0.27	0.0089(03)	0.206(12)	0.0295(16)	0.48	0.0506(28)	180±7	190±10	187±10
5#	1891	1251	0.66	0.0094(08)	0.207(11)	0.0298(14)	0.58	0.0508(23)	190±15	191±9	189±9
6#	1160	577	0.5	0.0091(08)	0.213(09)	0.0287(11)	0.61	0.0545(20)	184±17	196±8	182±7
7#	1960	2111	1.08	0.0096(04)	0.218(08)	0.0312(08)	0.62	0.0507(15)	192±8	200±7	198±5
8#*	990	226	0.23	0.0170(20)	0.281(21)	0.0290(19)	0.54	0.0703(47)	341±39	251±17	184±12
9#	1024	555	0.54	0.0086(06)	0.199(14)	0.0291(19)	0.57	0.0496(31)	173±12	185±12	185±12
10#	1286	981	0.76	0.0089(06)	0.201(05)	0.0292(05)	0.61	0.0504(11)	178±12	186±5	185±3
11#	1468	1141	0.78	0.0089(03)	0.211(08)	0.0306(08)	0.57	0.0499(16)	179±5	194±7	195±5
12#	1360	1110	0.82	0.0086(06)	0.195(06)	0.0291(06)	0.5	0.0491(13)	173±12	181±5	185±4
13#	443	179	0.4	0.0093(06)	0.179(06)	0.0279(05)	0.53	0.0471(14)	186±13	167±6	177±3
14#	722	324	0.45	0.0096(08)	0.179(12)	0.0262(13)	0.48	0.0500(30)	194±17	167±10	167±8
Sample 746											
1#	1000	442	0.44	0.0097(09)	0.217(17)	0.0292(14)	0.62	0.0525(32)	194±18	199±14	185±9
2#	408	107	0.26	0.0086(13)	0.194(20)	0.0293(12)	0.19	0.0481(51)	174±26	180±17	186±8
3#	469	51	0.11	0.0106(22)	0.196(21)	0.0274(10)	0.11	0.0517(56)	213±44	182±18	174±6
4#*	339	120	0.36	0.0119(15)	0.270(30)	0.0297(14)	0.13	0.0662(77)	238±31	243±24	189±9
5#*	559	120	0.21	0.0125(23)	0.237(29)	0.0255(14)	0.05	0.0676(91)	251±46	216±24	162±9
6#*	264	39	0.15	0.0110(19)	0.258(29)	0.0283(12)	0.05	0.0672(79)	222±39	233±23	180±8
7#*	249	76	0.31	0.0099(14)	0.245(30)	0.0284(12)	0.29	0.0618(72)	200±28	223±24	180±8
8#	305	109	0.36	0.0085(10)	0.197(24)	0.0276(10)	0.11	0.0515(62)	170±19	183±20	176±6
9#*	522	222	0.42	0.0124(15)	0.270(24)	0.0302(14)	0.25	0.0655(59)	250±29	243±19	192±9
10#*	365	171	0.47	0.0085(10)	0.233(25)	0.0292(12)	0.48	0.0565(53)	170±19	213±20	185±8
11#	1398	375	0.27	0.0081(11)	0.186(12)	0.0261(11)	0.30	0.0532(35)	164±22	173±11	166±7
12#*	549	140	0.25	0.0279(58)	0.401(43)	0.0282(14)	0.29	0.1064(110)	556±115	342±31	179±9
13#	410	122	0.30	0.0122(18)	0.194(22)	0.0268(11)	-0.09	0.0556(68)	225±35	180±18	170±7
14#*	263	100	0.38	0.0153(25)	0.402(56)	0.0296(14)	0.28	0.103(139)	306±51	343±42	188±9
15#*	192	27	0.14	0.0238(40)	0.300(39)	0.0291(15)	0.06	0.0795(108)	475±79	267±31	185±10
16#	585	176	0.30	0.0091(13)	0.200(18)	0.0280(13)	0.30	0.0539(48)	182±26	185±16	178±8
17#	1147	762	0.66	0.0077(09)	0.184(11)	0.0285(10)	0.14	0.0486(33)	154±18	172±10	181±7
18#	597	168	0.28	0.0076(12)	0.158(18)	0.0261(12)	0.05	0.0458(57)	153±23	149±16	166±8
19#	395	197	0.50	0.0087(22)	0.198(31)	0.0305(27)	0.36	0.0505(76)	175±43	183±27	194±17
20#	488	189	0.39	0.0092(12)	0.213(20)	0.0303(14)	0.25	0.0535(50)	186±25	196±17	192±9
21#	488	189	0.39	0.0092(12)	0.213(20)	0.0303(14)	0.25	0.0535(50)	186±25	196±17	192±9
22#	1457	1354	0.93	0.0079(09)	0.201(12)	0.0291(11)	0.26	0.0517(32)	160±18	186±11	185±7

U and Th concentrations are estimated from sensitivity factors calculated from GJ zircon (the Mainz crystal has 322 ppm U and 10.7 ppm Th). ^{204}Hg interferences on ^{204}Pb are subtracted using a $^{201}Hg/^{204}Hg$ ratio of 1.918. ^{235}U is calculated from ^{238}U using a $^{238}U/^{235}U$ ratio of 137.88. rho = error correlation defined as the quotient of the propagated errors of the $^{206}Pb/^{238}U$, $^{207}Pb/^{235}U$ and $^{207}Pb/^{206}Pb$ ratios. Uncertainties in parentheses are given for the last two digits and correspond to 1σ. * = Analysis not used for age calculation, due to irregular behavior of the ablation signal.

2011), or (ii) progressive depletion and metasomatism of a common melt source over the course of ophiolite formation (Shervais, 2001; Whattam and Stern, 2011). Overall, suprasubduction-zone settings encompass forearc, intraarc and backarc domains. On the basis of field relationships, such as (i) association with the coeval subduction-accretion complex, and (ii) presence of the Triassic intraoceanic subduction and accretion complex to the north, we favor a suprasubduction-zone forearc setting above a juvenile subduction zone.

Striking features of the Refahiye ophiolite in the studied part are (i) injection of the mantle section by hydrous basic magmas with suprasubduction-zone signature, and

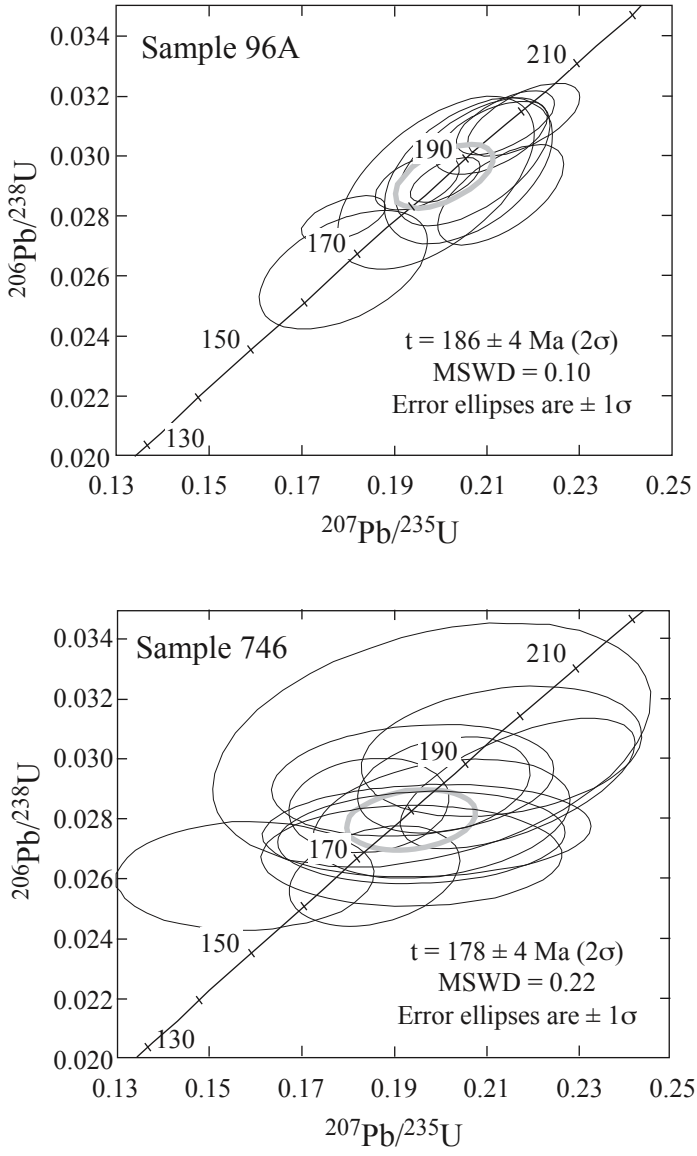

Fig. 11. Concordia diagrams of U-Pb zircon ages. Error ellipses are given at the 2 σ level. Concordia ages are calculated by Isoplot 3.50 (Ludwig, 2003).

(ii) local growth of relatively late hydrous minerals in mantle peridotites. Igneous intrusions into the deeper levels of oceanic crust and upper mantle are not rare phenomena seen in ophiolite complexes (for example, Moores and Vine, 1971; Karson, 1984; Nicolas, 1989; Malpas, 1990; Sarkarinejad, 2003). In the Refahiye ophiolite, grain sizes of the gabbroic stocks/dikes range from fine to medium, and there are locally dike through dike crosscutting relationships, suggesting several generations of dike injection. A similar case was documented in the Troodos ophiolite, and accounted for by the presence of multiple magma chambers related to intermit-

tent magmatic and tectonic activity (Malpas, 1990). Growth of the relatively late hydrous minerals in the peridotites, such as tremolite-hornblende, talc and chlorite as well as large-scale serpentinization can be tentatively attributed to the hydrothermal processes of injecting basic magma. There are two potential tectonic settings for dike intrusions into the mantle section: (i) very slowly spreading ridges or oceanic core complexes, and (ii) fracture zone consisting of three segments, a transform fault between two ridge ends and their non-transform extensions.

Apart from the local hydrothermal mineral growths in both peridotites and gabbros related to sea-floor hydrothermal metamorphism, rocks of the Refahiye ophiolite do not show any sign of regional metamorphism. We can thus eliminate the possibility that the Refahiye ophiolite was ever subducted. The associated metamorphic rocks include substantial oceanic material (for example, serpentinite, metachert, and metabasic rocks with enriched mid-ocean ridge basalt and ocean island basalt signatures; Topuz and others, 2013a; Göçmengil and others, 2013[2]). Both the greenschist-facies rocks (for example, Na-Ca amphibole and phengite) and high-grade blocks (eclogite, garnet amphibolite, and micaschist) contain mineral assemblages, suggesting metamorphism in a subduction zone. The field relations (see figs. 3 and 4), such as (i) association of the unsubducted suprasubduction-zone ophiolite with nearly coeval metamorphosed accretionary complexes, (ii) absence of any direct relationship to the southern Atlantic-type continental margin, represented by the Munzur limestones, and (iii) absence of any indication in the stratigraphic record of the southern Atlantic-type continental margin, the Menderes-Taurus block, for ophiolite obduction (fig. 2) clearly point to the emplacement of a trapped forearc ophiolite above its own subduction-accretion complex (fig. 12A). Thus, the Refahiye ophiolite differs from the "Late Cretaceous" ophiolite bodies and underlying ophiolitic mélanges, obducted onto the Munzur limestones, ~20 km to the south of the Refahiye ophiolite (fig. 3A; for example, Özgül and Turşucu, 1984). The location of the Refahiye ophiolite as the distal section of the Eastern Pontide continental margin atop a subduction-accretion complex requires that the ophiolite emplacement as a backstop along the Pacific-type continental margin occurred during early-medial Jurassic time. However, the oldest sedimentary rocks which discordantly overlie the Refahiye ophiolite and the associated metamorphic rocks in the studied transect are of early to medial Eocene age (figs. 3 and 4). There are local outcrops of late Jurassic–early Cretaceous calciturbidites (Kolaylı, ms, 1996), clearly overlying the Kop ophiolite (own observation), which is located roughly 30 km to the north east from the eastern end of the Refahiye ophiolite and occupies a similar tectonic position as the Refahiye ophiolite (fig. 1). This situation implies that the absence of older lithologies on the ophiolite and metamorphic rocks in the studied transect is probably related to uplift and erosion following the Paleocene–early Eocene continental collision between the Eastern Pontides and the Menderes-Taurus block. How far the original intraoceanic subduction was from the East Pontide margin during early Jurassic is unclear. It may be that the original subduction zone was farther away from the East Pontide margin and the Refahiye ophiolite plus its subduction-accretion cushion was emplaced by the elimination of a now vanished oceanic tract after Jurassic.

Common presence of the Jurassic ophirags within the Cretaceous ophiolitic mélanges (Dilek and Thy, 2006; Çelik and others, 2011, 2013; Göncüoğlu and others, 2012) and rarely preserved structurally intact Jurassic ophiolites (the Refahiye and Sevan ophiolites: this study; Galoyan and others, 2009; Hassig and others, 2013)

[2] Göçmengil, G., Altıntaş, İ. E., Topuz, G., Çelik, Ö. F., and Özkan, M., 2013, The diverse sources for the metaigneous rocks in the Jurassic metamorphosed accretionary complexes (Refahiye, NE Turkey): Geodinamica Acta, submitted.

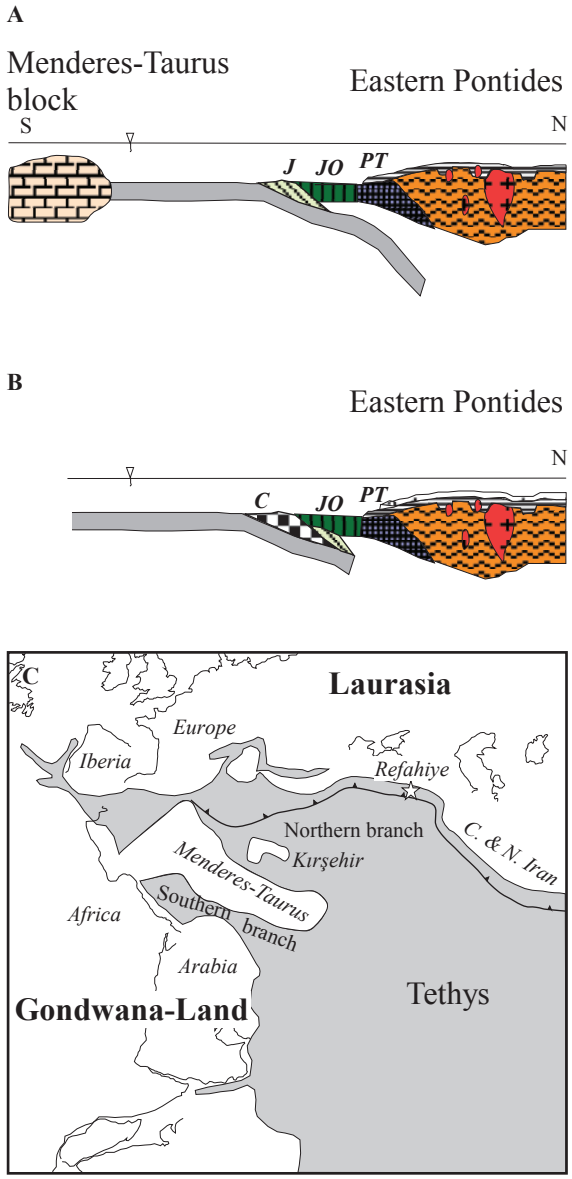

Fig. 12. (A) Schematic illustration of coeval formations of ophiolite and subduction-accretion complex. J: Jurassic accretionary complex; JO: Jurassic ophiolite; PT: Permo-Triassic accretionary complex. (B) Schematic illustration of the situation during the formation of Cretaceous ophiolitic mélange. Note that the Cretaceous ophiolitic mélange "C" is directly in contact with the Jurassic ophiolite. (C) Paleogeographic reconstruction for the Eastern Mediterranean region during the early Jurassic, and location of the inferred intraoceanic subduction zone. Relative positions of Laurasia and Gondwana-Land are after Barrier and Vrielynck (2008)

indicate that the ophiolite formation during Jurassic time was common along the IAE ocean similar to the Balkans. As pointed out above, early to medial Jurassic subduction-accretion complexes in the Refahiye area occur exclusively within the ophiolite, either beneath it or as tectonic slice within it, and do not have a contact with the late

Cretaceous ophiolitic mélange (figs. 3 and 4). This field relationship implies that accretion was not continuous from early Jurassic to late Cretaceous time (fig. 12B). In case of continuous subduction and accretion, it is expected that subduction-accretion complex displays gradual younging towards the trench, as documented in the Franciscan complex (Wakabayashi and others, 2010; Wakabayashi, 2013, and the references therein). This field relationship can be accounted for by (i) non-existence of a late Jurassic subduction due to the Cimmerian collision (preferred by Şengör), or removal of the trenchward domains of subduction-accretion complex and overlying ophiolite by (ii) a strike-slip fault or (iii) subduction erosion (preferred by Topuz). On the basis of absence of a definable continental fragment between the subduction-accretion complexes of different ages, Topuz and others (2013a) inferred episodic accretionary growth of the southern margin of the Pontides from Late Paleozoic to end-Mesozoic without involvement of Cimmerian ribbon continent (The third author, A. M. C. Şengör disagrees with this view). As so far no strike-slip activity apart from the active NAF has been documented close to the IAES, removal by strike-slip fault is regarded as unlikely. Subduction erosion (the third possibility) has been recognized as the main process for the removal of the upper plate material (for example, von Huene and Scholl, 1991; Kukowski and Oncken, 2006), and diminish the width of the previously accreted material (in our case Jurassic subduction-accretion complex and overlying suprasubduction-zone ophiolite). Field geological evidence for the operation of the subduction erosion is provided by the northward migration of the magmatic arc fronts during early-medial Jurassic and late Cretaceous times (see Okay and Şahintürk, 1997). Whether the dismemberment of the Jurassic ophiolites and their incorporation into the Cretaceous ophiolitic mélanges in form of ophirags occurred during subduction erosion or during a separate event is an open question.

The key problem now has become why the Jurassic ophiolites in the Balkans were obducted onto an Atlantic-type continental margin and the Refahiye ophiolite remained as a forearc backstop atop a developing subduction-accretion complex along a Pacific-type continental margin. In the eastern Mediterranean region, the main Tethyan sutures are represented by the Vardar suture in the Balkans, and the Intra-Pontide, the İzmir-Ankara-Erzincan, the Inner Tauride and the Bitlis sutures in Turkey (fig. 1). Existence of another suture, the so-called Pindos-Mirdita, is highly contentious (compare, Robertson, 2012; Ferriere and others, 2012). Closure of both the Vardar and İzmir-Ankara-Erzincan oceans is thought to have occurred during early Tertiary time (Şengör and Yılmaz, 1981; Okay and Şahintürk, 1997; Rolland and others, 2009b; Sosson and others, 2010; Robertson, 2012). The late Jurassic ophiolite obduction over the Pelagonian zone in the Balkans can be traced into Sporades islands in the Aegean Sea, and Late Cretaceous ophiolite obduction onto Menderes-Taurus block is not observed to the west of the Bornova flysch zone (fig. 1) (Okay and others, 2012, and the references therein). Unlike the Balkans, there is no indication for ophiolite obduction in the stratigraphic record of the Menderes-Taurus block during late Jurassic to early Cretaceous time (fig. 3). During the early Jurassic, Tethys formed a westerly narrowing embayment between the Laurasia and Apulia, a continental block partly detached from the Gondwana-Land (fig. 12C; Şengör and Natal'in, 1996; Barrier and Vrielynck, 2008). Such a paleogeographic reconstruction requires that the distance between the Laurasia and the Apulia was shorter relative to that in the east. Based on this argument, we hypothesize that the intra-oceanic subduction zone was located close to the southern Atlantic-type continental margin in the Balkans and far away in Turkey and farther east during early to medial Jurassic time (fig. 12C). In this situation, further subduction would lead to ophiolite obduction over the Atlantic-type continental margin in the west, and to the growth of the accretionary wedge in the east. Increase in the amount of accreted material beneath the ophiolite would eventually

result in the gravitational collapse of ophiolite, to be obducted onto its own Pacific-type continental margin. In the Balkans, ophiolite obduction during the late Jurassic over the Atlantic-type continental margin requires initiation of another subduction zone in the oceanic domain in the north. Consequently, a late Cretaceous accretionary prism locally overrides the former passive margin with its earlier obducted (Jurassic) ophiolites, as in Kozara area (northern Bosnia and Herzegovina) (Ustaszewski and others, 2009, 2010). This situation is comparable with that in Oman. During the late Cretaceous, ophiolite obduction took place over the Oman, and subduction along a different subduction zone is still ongoing beneath the Makran (Searle and Cox, 1999).

CONCLUSIONS

The Refahiye ophiolite with a length of ~175 km and width of ~20 km forms one of the biggest ophiolite bodies occurring between the Eastern Pontides and the Menderes-Taurus block in northern Turkey. The ophiolite is represented mainly by mantle peridotites locally crosscut by gabbroic intrusions with suprasubduction-zone affinities. U-Pb zircon and published Ar-Ar hornblende ages are consistently indicative of an ophiolite formation during early Jurassic time. Presence of rarely preserved structurally intact ophiolites (the Refahiye ophiolite) together with the reported widespread presence of Jurassic ophirags in Cretaceous ophiolitic mélanges reveals that Jurassic oceanic spreading was widespread along the İzmir-Ankara-Erzincan ocean, similar to the Balkans. Several lines of evidence such as (i) close association with coeval oceanic accretionary complexes, (ii) absence of any direct relationship to the southern Atlantic-type continental margin (the Menderes-Taurus block), and (iii) absence of any indication in the stratigraphic record of the southern Atlantic-type continental margin for ophiolite emplacement during Jurassic time, conclusively suggest emplacement of a trapped forearc ophiolite above its own subduction-accretion complex as a backstop. Striking difference in mode of emplacement (obduction over the leading edge of the Atlantic-type continental margin vs. emplacement of a forearc ophiolite above its own subduction-accretion complex at the Pacific-type continental margin) between the Eo-Hellenic ophiolites and the Refahiye ophiolite was probably a function of the distance of the intra-oceanic subduction zone to the Atlantic-type continental margins for example, Pelagonia in the Balkans and Menderes-Taurus block in Turkey. Rarity of the structurally intact Jurassic ophiolites in Turkey is related to the later removal by subduction erosion and dismemberment by tectonic processes from the upper plate of the subduction zone and incorporation into Cretaceous ophiolitic mélanges.

ACKNOWLEDGMENTS

This work was financially supported by a research grant from the Scientific and Technological Research Council of Turkey (TÜBITAK #109Y059), and partial support from the Turkish Academy of Sciences (TÜBA) Young Scientists Award Program (GEBIP) as well as the Istanbul Technical University Research Foundation (İTÜ-BAP). We gratefully acknowledge the fruitful discussions with Aral I. Okay, Boris Natal'in, Gürsel Sunal and Ali Yılmaz, the thin section preparation by Mehmet Ali Oral, Ilona Fin and Oliver Wienand, help of Mutlu Özkan during field work, and helps of Erkan Aydar, H. Evren Çubukçu and Lütfiye Akın during CL-imaging of zircons. John F. Dewey most kindly kept us up-to-date on fracture zone origin of ophiolites and boninite generation. The manuscript benefited from helpful reviews by John Wakabayashi and Alastair H. F. Robertson. We thank Associate Editor David A. D. Evans for painstaking editorial handling.

References

Agard, P., Jolivet, L., Vrielynck, B., Burov, E., and Monie, P., 2007, Plate accelaration: The obduction trigger?: Earth and Planetary Science Letters, v. 258, n. 3–4, p. 428–441, http://dx.doi.org/10.1016/j.epsl.2007.04.002

Akal, C., Candan, O., Koralay, O. E., Oberhansli, R., Chen, F., and Prelevic, D., 2012, Early Triassic potassic volcanism in the Afyon Zone of the Anatolides/Turkey: implications for the rifting of the Neo-Tethys: International Journal of Earth Sciences, v. 101, n. 1, p. 177–194, http://dx.doi.org/10.1007/s00531-011-0654-2

Akbaş, B., Akdeniz, N., Aksay, A., Altun, İ. E., Balcı, V., Bilginer, E., Bilgiç, M., Duru, M., Ercan, T., Gedik, İ., Günay, Y., Güven, İ. H., Hakyemez, H. Y., Konak, N., Papak, İ., Pehlivan, Ş., Sevin, M., Şenel, M., Tarhan, N., Turhan, N., Türkecan, A., Ulu, Ü., Uğuz, M., and F., Yurtsever, A., 2011, Geological map of Turkey: Ankara, Maden Tetkik ve Arama Genel Müdürlüğü, scale 1:500,000.

Barrier, E., and Vrielynck, B., 2008, Palaeotectonic maps of the Middle East: Tectono-sedimentary-Palinspatic maps from Late Norian to Pliocene: Paris, Commission for the Geological *Map* of the World (*CGMW*)/UNESCO (http://www.ccgm.org) Atlas of 14 *maps*, scale 1/18 500 000.

Bergougnan, H., 1975, Relations entre les édifices pontique et taurique dans le Nord-Est de l'Anatolie: Bulletin de la Société Géologique de France, series 7, v. 17, p. 1045–1057.

——— ms, 1986, Etudes geologiques dans l'est—Anatolien: Paris, France, I'Universite Pierre et Marie Curie, Ph. D. thesis, Paris, 606 p.

Bernoulli, D., and Laubscher, H., 1972, The palinspastic problem of the Hellenides: Eclogae Geologicae Helvetiae, v. 65, n. 1, p. 107–118.

Boynton, W. V., 1984, Cosmochemistry of the rare earth elements: meteorite studies, *in* Henderson, P., editor, Rare earth element geochemistry: Amsterdam, Elsevier, p. 63–114.

Boztuğ, D., and Harlayan, Y., 2008, K-Ar ages of granitoids unravel the stages of Neo-Tethyan convergence in the eastern Pontides and central Anatolia, Turkey: International Journal of Earth Sciences, v. 97, n. 3, p. 585–599, http://dx.doi.org/10.1007/s00531-007-0176-0

Candan, O., Koralay, O. E., Akal, C., Kaya, O., Oberhansli, R., Dora, O. Ö., Konak, N., and Chen, F., 2011, Supra-Pan-African unconformity between core and cover series of the Menderes Massif/Turkey and its geological implications: Precambrian Research, v. 184, n. 1–4, p. 1–23, http://dx.doi.org/10.1016/j.precamres.2010.09.010

Casey, J. F., and Dewey, J. F., 1984, Initiation of subduction zones along transform and accreting plate boundaries, triple-junction evolution, and forearc spreading centres—implications for ophiolite geology and obduction, *in* Grass, I. G., Lippard, S. J., and Shelton, A. W., editors, Ophiolites and oceanic lithosphere: Geological Society, London, Special Publications, v. 13, p. 269–290, http://dx.doi.org/10.1144/GSL.SP.1984.013.01.22

Çelik, Ö. F., Delaloye, M., and Feraud, G., 2006, Precise ^{40}Ar-^{39}Ar ages from the metamorphic sole rocks of the Tauride Belt ophiolites, southern Turkey: implications for the rapid cooling history: Geological Magazine, v. 143, n. 2, p. 213–227, http://dx.doi.org/10.1017/S0016756805001524

Çelik, Ö. F., Marzolli, A., Marschik, R., Chiaradia, M., Neubauer, F., and Öz, I., 2011, Early-Middle Jurassic intra-oceanic subduction in the İzmir-Ankara-Erzincan ocean, Northern Turkey: Tectonophysics, v. 509, n. 1–2, p. 120–134, http://dx.doi.org/10.1016/j.tecto.2011.06.007

Çelik, Ö. F., Chiaradia, M., Marzoli, A., Billor, Z., and Marschik, R., 2013, The Eldivan ophiolite and volcanic rocks in the İzmir-Ankara-Erzincan suture zone, northern Turkey: Geochemistry, whole-rock geochemical and Nd-Sr-Pb isotopic characteristics: Lithos, v. 172–173, p. 31–46, http://dx.doi.org/10.1016/j.lithos.2013.03.010

Chan, G. H.-N., Malpas, J., Xenophontos, C., and Lo, C.-H., 2007, Timing of subduction zone metamorphism during the formation and emplacement of Troodos and Baër-Bassit ophiolites: Insights from 40Ar–39Ar geochronology: Geological Magazine, v. 144, n. 5, p. 797–810, http://dx.doi.org/10.1017/S0016756807003792

Cherniak, D. J., and Watson, E. B., 2000, Pb diffusion in zircon: Chemical Geology, v. 172, n. 1–2, p. 5–24, http://dx.doi.org/10.1016/S0009-2541(00)00233-3

Choi, S. H., Shervais, J. W., and Mukasa, S. B., 2008, Supra-subduction and abyssal mantle peridotites of the Coast range ophiolite, California: Contributions to Mineralogy and Petrology, v. 156, n. 5, p. 551–576, http://dx.doi.org/10.1007/s00410-008-0300-6

Coleman, R. G., 1971, Plate tectonic emplacement of upper mantle peridotites along continental edges: Journal of Geophysical Research, v. 76, n. 10, p. 1212–1222, http://dx.doi.org/10.1029/JB076i005p01212

——— 2000, Prospecting for ophiolites along the California continental margin, *in* Dilek, Y., Moores, E., Elthon, D., and Nicolas, A., editors, Ophiolites and oceanic crust: new insights from field studies and the Ocean Drilling Program: Geological Society of America Special Papers, v. 349, p. 351–364, http://dx.doi.org/10.1130/0-8137-2349-3.351

Dewey, J. F., 1976, Ophiolite obduction: Tectonophysics, v. 31, n. 1–2, p. 93–120, http://dx.doi.org/10.1016/0040-1951(76)90169-4

——— 2003, Ophiolites and lost oceans: rifts, ridges, arcs, and/or scrapings, *in* Dilek, Y., and Newcomb, S., editors, Ophiolite concept and the evolution of geological thought: Geological Society of America Special Papers, v. 373, p. 153–158, http://dx.doi.org/10.1130/0-8137-2373-6.153

Dewey, J. F., and Bird, J. M., 1971, Origin and emplacement of the ophiolite suite: Appalachian ophiolites in Newfoundland: Journal of Geophysical Research, v. 76, n. 14, p. 3179–3206, http://dx.doi.org/10.1029/JB076i014p03179

Dewey, J. F., and Casey, J. F., 2011, The origin of obducted large-slab ophiolite complexes, *in* Brown, D., and Ryan, P. D., editors, Arc-continent collision: Berlin, Heidelberg, Springer-Verlag, p. 431–444.

Dick, H. J. B., and Bullen, T., 1984, Chromian spinel as a petrogenetic indicator in abyssal and Alpine-type

peridotites and spatially associated lavas: Contributions to Mineralogy and Petrology, v. n. 1, 86, p. 54–76, http://dx.doi.org/10.1007/BF00373711
Dilek, Y., and Thy, P., 2006, Age and petrogenesis of plagiogranite intrusions in the Ankara mélange, central Turkey: Island Arc, v. 15, n. 1, p. 44–57, http://dx.doi.org/10.1111/j.1440-1738.2006.00522.x
——— 2009, Island arc tholeiite to boninitic melt evolution of the Cretaceous Kızıldağ (Turkey) ophiolite: Model for multi-stage early arc-forearc magmatism in Tethyan subduction factories: Lithos, v. 113, n. 1–2, p. 68–87, http://dx.doi.org/10.1016/j.lithos.2009.05.044
Dilek, Y., and Whitney, D. L., 1997, Counterclockwise *P-T-t* trajectory from the metamorphic sole of a Neo-Tethyan ophiolite (Turkey): Tectonophysics, v. 280, n. 3–4, p. 295–310, http://dx.doi.org/10.1016/S0040-1951(97)00038-3
Dilek, Y., Thy, P., Hacker, B., and Grundvig, S., 1999, Structure and petrology of Tauride ophiolites and mafic dike intrusions (Turkey): Implications for the Neotethyan ocean: Geological Society of America Bulletin, v. 111, n. 8, p. 1192–1216, http://dx.doi.org/10.1130/0016-7606(1999)111⟨1192:SAPOTO⟩2.3.CO;2
Dimo-Lahitte, A., Monié, P., and Vergély, P., 2001, Metamorphic soles from the Albanian ophiolites: Petrology, $^{40}Ar/^{39}Ar$ geochronology, and geodynamic evolution: Tectonics, v. 20, n. 1, p. 78–96, http://dx.doi.org/10.1029/2000TC900024
Dokuz, A., 2011, A slab detachment and delamination model for the generation of Carboniferous high-potassium I-type magmatism in the Eastern Pontides, NE Turkey: The Köse composite pluton: Gondwana Research, v. 19, n. 4, p. 926–944, http://dx.doi.org/10.1016/j.gr.2010.09.006
Dokuz, A., Karslı, O., Chen, B., and Uysal, İ., 2010, Sources and petrogenesis of Jurassic granitoids in the Yusufeli area, Northeastern Turkey: Implications for pre- and post-collisional lithospheric thinning of the eastern Pontides: Tectonophysics, v. 480, n. 1–4, p. 259–279, http://dx.doi.org/10.1016/j.tecto.2009.10.009
Ferriére, J., Chanier, F., and Ditbanjong, P., 2012, The Hellenic ophiolites: eastward or westward obduction of the Maliac Ocean, a discussion: International Journal of Earth Sciences, v. 101, n. 6, p. 1559–1580, http://dx.doi.org/10.1007/s00531-012-0797-9
Galoyan, G., Rolland, Y., Sosson, M., Corsini, M., Billo, S., Verati, C., and Melkonyan, R., 2009, Geology, geochemistry and $^{40}Ar–^{39}Ar$ dating of Sevan ophiolites (Lesser Caucasus, Armenia): Evidence for Jurassic back-arc opening and hot spot event between the south Armenian block and Eurasia: Journal of Asian Earth Sciences, v. 34, n. 2, p. 135–153, http://dx.doi.org/10.1016/j.jseaes.2008.04.002
Genç, Ş. C., and Tüysüz, O., 2010, Tectonic setting of the Jurassic bimodal magmatism in the Sakarya Zone (Central and Western Pontides), Northern Turkey: A geochemical and isotopic approach: Lithos, v. 118, n. 1–2, p. 95–111, http://dx.doi.org/10.1016/j.lithos.2010.03.017
Göncüoğlu, M. C., Marroni, M., Sayit, K., Tekin, U. K., Ottria, G., Pandolfi, L., and Ellero, A., 2012, The Aylı Dağ ophiolite sequence (Central Northern Turkey): A fragment of Middle Jurassic oceanic lithosphere within the Intra-Pontide suture zone: Ofioliti, v. 37, n. 2, p. 77–92, http://dx.doi.org/10.4454/ofioliti.v37i2.407
Görür, N., Şengör, A. M. C., Akkök, R., and Yılmaz, Y., 1983, Pontidlerde Neotetisin kuzey kolunun açılmasına ilişkin sedimentolojik veriler: Türkiye Jeoloji Kurumu Bülteni, v. 26, p. 11–20.
Görür, N., Tüysüz, O., Aykol, A., Sakınç, M., Yiğitbaş, E., and Akkök, R., 1993, Cretaceous red pelagic carbonates of northern Turkey: Their place in the opening history of the Black Sea: Eclogae Geologicae Helvetiae, v. 86, n. 3, p. 819–838.
Hamilton, W., 1979, Tectonics of the Indonesian region: United States Geological Survey Professional Paper 1078, 345 p.
Harris, N. B., Kelley, S., and Okay, A. I., 1994, Post-collision magmatism and tectonics in northwest Anatolia: Contributions to Mineralogy and Petrology, v. 117, n. 3, p. 241–252, http://dx.doi.org/10.1007/BF00310866
Hässig, M., Rolland, Y., Sosson, M., Galoyan, G., Müller, C., Avagyan, A., and Sahakyan, L., 2013, New structural and petrological data on the Amasia ophiolites (NW Sevan–Akera suture zone, Lesser Caucasus): Insights for a large-scale obduction in Armenia and NE Turkey: Tectonophysics, v. 588, p. 135–153, http://dx.doi.org/10.1016/j.tecto.2012.12.003
Hatzipanagiotou, K., and Pe-Piper, G., 1995, Ophiolitic and sub-ophiolitic metamorphic rocks of the Vatera area, southern Lesbos (Greece): geochemistry and geochronology: Ofioliti, v. 20, p. 17–29.
Hebert, R., Adamson, A. C., and Komor, S. C., 1990, Metamorphic petrology of ODP 109, Hole 670A serpentinized peridotites. Serpentinization at slow spreading ridge environment, *in* Detrick, R., Honnorez, J., Bryan, W. B., Juteau, and others, editors, Scientific Results: Proceeding of the Ocean Drilling Program, v. 106/109, p. 103–115.
Hoskin, P. W. O., and Schaltegger, U., 2003, The composition of zircon and igneous and metamorphic petrogenesis, *in* Hanchar, J. M., and Hoskin, P. W. O., editors, Zircon: Reviews in Mineralogy and Geochemistry, v. 53, p. 27–62, http://dx.doi.org/10.2113/0530027
Ishii, T., Robinson, P. T., Maekawa, H., and Fiske, R., 1992, Petrological studies of peridotites from diapiric serpentinite seamounts in the Izu-Ogazawa-Mariana forearc, Leg 125, *in* Fryer, P., Pearce, J. A., Stokking, L. B., and others, editors, Scientific Results: Proceedings in the Ocean Drilling Program, v. 125, p. 445–485.
Jacobshagen, V., 1986, Geologie von Griechenland: Berlin-Stuttgart, Gebrüder Borntraeger, 363 p.
Johnson, K. T. M., Dick, H. J. B., and Shimizu, N., 1990, Melting in the oceanic upper mantle: An ion microprobe study of diopsides in abyssal peridotites: Journal of Geophysical Research—Solid Earth, v. 95, n. B3, p. 2661–2678, http://dx.doi.org/10.1029/JB095iB03p02661
Kandemir, R., and Yılmaz, C., 2009, Lithostratigraphy, facies, and deposition environment of the lower Jurassic ammonitico rosso type sediments (ARTS) in the Gümüşhane area, NE Turkey: Implications for

the opening of the northern branch of the Neo-Tethys ocean: Journal of Asian Earth Sciences, v. 34, n. 4, p. 586–598, http://dx.doi.org/10.1016/j.jseaes.2008.08.006
Karrig, D. E., Lawrence, M. B., Moore, G. F., and Curray, J. R., 1980, Structural framework of the forearc basin, NW Sumatra: Journal of the Geological Society, London, v. 137, n. 1, p. 77–91, http://dx.doi.org/10.1144/gsjgs.137.1.0077
Karson, J. A., 1984, Variations in structure and petrology in the Coastal Complex, Newfoundland: anatomy of an oceanic fracture zone, *in* Grass, I. G., Lippard, S. J., and Shelton, A. W., editors, Ophiolites and oceanic lithosphere: Geological Society, London, Special Publications, v. 13, p. 131–144, http://dx.doi.org/10.1144/GSL.SP.1984.013.01.12
Kaygusuz, A., Arslan, M., Siebel, W., Sipahi, F., and İlbeyli, N., 2012, Geochronological evidence and tectonic significance of Carboniferous magmatism in the southwest Trabzon area, eastern Pontides, Turkey: International Geology Review, v. 54, n. 15, p. 1776–1800, http://dx.doi.org/10.1080/00206814.2012.676371
Ketin, İ., 1966, Anadolu'nun tektonik birlikleri: Maden Tetkit ve Arama Dergisi, v. 66, p. 20–34.
Khalatbari-Jafari, M., Juteau, T., Bellon, H., Whitechurch, H., Cotten, J., and Emami, H., 2004, New geological, geochronological and geochemical investigations on the Khoy ophiolites and related formations, NW Iran: Journal of Asian Earth Sciences, v. 23, n. 4, p. 507–535, http://dx.doi.org/10.1016/j.jseaes.2003.07.005
Koch, R., Bucur, I. I., Kırmacı, M. Z., Eren, M., and Taslı, K., 2008, Upper Jurassic and Lower Cretaceous carbonate rocks of the Berdiga Limestone—Sedimentation on an onbound platform with volcanic and episodic siliciclastic influx. Biostratigraphy, facies and diagenesis (Kircaova, Kale-Gümüşhane area; NE-Turkey): Neues Jahrbuch für Geologie und Paläontologie Abhandlungen, v. 247, n. 1, p. 23–61, http://dx.doi.org/10.1127/0077-7749/2008/0247-0023
Koepke, J., Seidel, E., and Kreuzer, H., 2002, Ophiolites on the Southern Aegean islands Crete, Karpathos and Rhodes: composition, geochronology and position within the ophiolite belts of the Eastern Mediterranean: Lithos, v. 65, n. 1–2, p. 183–203, http://dx.doi.org/10.1016/S0024-4937(02)00165-2
Kolaylı, H., ms, 1996, Kop Dağları (Erzincan-Erzurum-Bayburt) ultramafik ve mafik kayaçların jeolojik, petrolojik ve metalojik incelemesi: Trabzon, Turkey, Karadeniz Teknik Üniversitesi, Ph. D. thesis, 282 p.
Konak, N., Hakyemez, H. Y., Bilgiç, T., Bilgin, R., Hepşen, N., and Ercan, T., 2001, Kuzeydoğu Pontidler'in (Oltu-Olur-Şenkaya-Narman-Uzundere-Yusufeli) Jeolojisi: Ankara, Turkey, Maden Tetkik ve Arama, Rapor 10489.
Koralay, O. E., Satır, M., and Dora, O. Ö., 2001, Geochemical and geochronological evidence for Early Triassic calc-alkaline magmatism in the Menderes Massif, western Turkey: International Journal of Earth Sciences, v. 89, n. 4, p. 822–835, http://dx.doi.org/10.1007/s005310000134
Kröner, A., and Şengör, A. M. C., 1990, Archean and Proterozoic ancestry in late Precambrian to early Paleozoic crustal elements of southern Turkey as revealed by single-zircon dating: Geology, v. 18, n. 12, p. 1186–1190, http://dx.doi.org/10.1130/0091-7613(1990)018⟨1186:AAPAIL⟩2.3.CO;2
Kukowski, N., and Oncken, O., 2006, Subduction erosion—the normal mode of fore-arc material transfer along the Chilean margin?, *in* Oncken, O., Chong, G., Franz, G., Giese, P., Gotze, H.-J., Ramos, V., Strecker, M., and Wigger, P., editors, The Andes active subduction orogeny: Berlin-Heidelberg, Springer Verlag, Frontiers in Earth Science, ch. 10, p. 217–236.
Kusky, T. M., Glass, A., and Tucker, R., 2007, Structure, Cr-chemistry, and the age of the Border Ranges ultramafic-mafic complex: A suprasubduction-zone ophiolite complex, *in* Ridgway, K. D., Trop, J. M., Glen, J. M. G., and O'Neill, J. M., editors, Tectonic growth of a collisional continental margin: crustal evolution of southern Alaska: The Geological Society of America Special Papers, v. 431, p. 207–225, http://dx.doi.org/10.1130/2007.2431(09)
Lanphere, M. A., Coleman, R. G., Karamata, S., and Pamić, J., 1975, Age of amphibolites associated with Alpine peridotites in the Dinaride ophiolite zone, Yugoslavia: Earth and Planetary Science Letters, v. 26, n. 3, p. 271–276, http://dx.doi.org/10.1016/0012-821X(75)90001-1
Lee, J. K. W., Williams, I. S., and Ellis, D. J., 1997, Pb, U and Th diffusion in natural zircon: Nature, v. 390, p. 159–161, http://dx.doi.org/10.1038/36554
Liati, A., Gebauer, D., and Fanning, C. M., 2004, The age of ophiolitic rocks of the Helenides (Vourinos, Pindos, Crete): first U-Pb ion microprobe (SHRIMP) zircon ages: Chemical Geology, v. 207, n. 3–4, p. 171–188, http://dx.doi.org/10.1016/j.chemgeo.2004.02.010
Ludwig, K. R., 2003, Isoplot/Ex 3.00. A geochronological toolkit for Microsoft Excel: Berkley Geochronological Center, Special Publication No. 4, 70 p.
Malpas, J., 1990, Crustal accretionary processes in the Troodos ophiolite, Cyprus: Evidence from field mapping and deep crustal drilling, *in* Malpas, J., Moores, E. M., Panayiotou, A., and Xenophontos, S., editors, Ophiolites, oceanic crustal analogues: Nicosia, Cyprus, Geological Survey Department, p. 63–74.
Miyashiro, A., 1973, The Troodos complex was probably formed in an island arc: Earth and Planetary Science Letters, v. 19, n. 2, p. 218–224, http://dx.doi.org/10.1016/0012-821X(73)90118-0
Moix, P., Beccaletto, L., Kozur, H. W., Hochard, C., Rosselet, F., and Stampfli, G. M., 2008, A new classification of the Turkish terranes and sutures and its implication for the paleotectonic history of the region: Tectonophysics, v. 451, n. 1–4, p. 7–39, http://dx.doi.org/10.1016/j.tecto.2007.11.044
Moores, E. M., 1982, Origin and emplacement of ophiolites: Reviews of Geophysics and Space Physics, v. 20, n. 4, p. 735–760, http://dx.doi.org/10.1029/RG020i004p00735
Moores, E. M., and Vine, F. J., 1971, The Troodos Massif, Cyprus and other ophiolites as oceanic crust; evaluation and implications: Philosophical Transactions of the Royal Society of London, Series A, v. 268, n. 1192, p. 443–466, http://dx.doi.org/10.1098/rsta.1971.0006
Nicolas, A., 1989, Structures of ophiolites and dynamics of oceanic lithosphere: Dordrecht, Kluwer Academic Publishers, 367 p.

Ogg, J. G., Ogg, G., and Gradstein F. M., 2008, The concise geologic time scale: New York, Cambridge University Press, 184 p.

Okay, A. I., 1984, The geology of the Ağvanis metamorphic rocks and neighboring formations: Bulletin of the Mineral Research and Exploration Institute of Turkey, v. 99/100, p. 16–36.

Okay, A. I., and Leven, E. Ja., 1996, Stratigraphy and paleontology of the Upper Paleozoic sequence in the Pulur (Bayburt) region, Eastern Pontides: Turkish Journal of Earth Sciences, v. 5, p. 145–155.

Okay, A. I., and Şahintürk, Ö., 1997, Geology of the Eastern Pontides, *in* Robinson, A. G., editor, Regional and petroleum geology of the black sea and surrounding region: American Association of Petroleum Geologists Memoir 68, p. 291–311.

Okay, A. I., and Tüysüz, O., 1999, Tethyan sutures of northern Turkey, *in* Durand, B., Jolivet, L., Horvath, F. F., and Seranne, M., editors, The Mediterranean Basins: Tertiary extension within the Alpine orogen: Geological Society, London, Special Publications, v. 156, p. 475–515, http://dx.doi.org/10.1016/10.1144/GSL.SP.1999.156.01

Okay A. I., Tansel, İ., and Tüysüz, O., 2001, Obduction, subduction and collision as reflected in the Upper Cretaceous-Lower Eocene sedimentary record of western Turkey: Geological Magazine, v. 138, n. 2, p. 117–142, http://dx.doi.org/10.1017/S0016756801005088

Okay, A. I., İşintek, İ., Altıner, D., Özkan-Altıner, S., and Okay, N., 2012, An olistostrome-melánge belt formed along a suture: Bornova flysch zone, western Turkey: Tectonophysics, v. 568–569, p. 282–295, http://dx.doi.org/10.1016/j.tecto.2012.01.007

Önen, A. P., 2003, Neotethyan ophiolitic rocks of the Anatolides of NW Turkey and comparison with Tauride ophiolites: Journal of the Geological Society, London, v. 160, n. 6, p. 947–962, http://dx.doi.org/10.1144/0016-764902-125

Önen, A. P., and Hall, R., 2000, Sub-ophiolite metamorphic rocks from NW Anatolia, Turkey: Journal of Metamorphic Geology, v. 18, n. 5, p. 483–495, http://dx.doi.org/10.1046/j.1525-1314.2000.00276.x

Özgül, N., and Turşucu, A., 1984, Stratigraphy of the Mesozoic carbonate sequence of the Munzur Mountains (Eastern Taurides), *in* Tekeli, O., and Göncüoğlu, M. C., editors, Geology of the Taurus Belt: Ankara, Maden Tetkik Arama Enstitüsü, p. 173–181.

Parlak, O., and Delaloye, M., 1999, Precise $^{40}Ar^{39}Ar$ ages from the metamorphic sole of the Mersin ophiolite (Southern Turkey): Tectonophysics, v. 301, n. 1–2, p. 145–158, http://dx.doi.org/10.1016/S0040-1951(98)00222-4

Parlak, O., Karaoğlan, F., Rızaoğlu, T., Klötzli, U., Koller, F., and Billor, B., 2013a, U-Pb, ^{40}Ar-^{39}Ar geochronology of the ophiolites and granitoids from the Tauride belt: Implications for the evolution of the Inner Tauride suture: Journal of Geodynamics, v. 65, p. 22–37, http://dx.doi.org/10.1016/j.jog.2012.06.012

Parlak, O., Çolakoğlu, A., Dönmez, C., Sayak, H., Yıldırım, N., Türkel, A., and Odabaşı, İ., 2013b, Geochemistry and tectonic significance of ophiolites along the Izmir-Ankara-Erzincan suture zone in northeastern Anatolia, *in* Robertson, A. H. F., Parlak, O., and Ünlügenç, U. C., editors, Geological development of Anatolia and the easternmost Mediterranean region: Geological Society, London, Special Publications, v. 372, p. 75–105, http://dx.doi.org/10.1144/SP372.7

Pearce, J. A., Lippard, S. L., and Roberts, S., 1984, Characteristics and tectonic significance of supra-subduction zone ophiolites, *in* Kokelaar, B. P., and Howells, M. F., editors, Marginal Basin Geology: Volcanic and associated sedimentary and tectonic Processes in modern and ancient marginal basins: Geological Society, London, Special Publications, v. 16, p. 77–94, http://dx.doi.org/10.1144/GSL.SP.1984.016.01.06

Pelin, S., 1977, Geological study of the area southeast of Alucra (Giresun), with special reference to its petroleum potential (in Turkish): Trabzon, Karadeniz Teknik Üniversitesi Yayını 87, 103 p.

Rice, S. P., Robertson, A. H. F., and Ustaömer, T., 2006, Late Cretaceous-Early Cenozoic tectonic evolution of the Eurasian active margin in the Central and eastern Pontides, northern Turkey, *in* Robertson, A. H. F., and Mountrakis, D., editors, Tectonic development of the eastern Mediterranean region: Geological Society, London, Special Publications, v. 260, p. 413–445, http://dx.doi.org/10.1144/GSL.SP.2006.260.01.17

Rice, S. P., Robertson, A. H. F., Ustaömer, T., Inan, N., and Taslı, K., 2009, Late Cretaceous-Early Eocene tectonic development of the Tethyan suture zone in the Erzincan area, Eastern Pontides, Turkey: Geological Magazine, v. 146, n. 4, p. 567–590, http://dx.doi.org/10.1017/S0016756809006360

Ricou, L. E., Argyriadis, I., and Marcoux, J., 1975, L'Axe Calcaire du Taurus, un alignement de fenetres arabo-africaines sous des nappes radiolaritiques, ophiolitiques et metamorphiques: Bulletin de la Société géologique de France, series 7, v. 17, p. 1024–1043.

Robertson, A. H. F., 2002, Overview of the genesis and emplacement of the Mesozoic ophiolites in the Eastern Mediterranean Tethyan region: Lithos, v. 65, n. 1–2, p. 1–67, http://dx.doi.org/10.1016/S0024-4937(02)00160-3

——— 2006, Contrasting modes of ophiolite emplacement in the Eastern Mediterranean region, *in* Gee, D. G., and Stephenson, R. A., editors, European Lithosphere Dynamics: Geological Society, London, Memoirs, v. 32, p. 235–261, http://dx.doi.org/10.1144/GSL.MEM.2006.032.01.14

——— 2012, Late Paleozoic-Cenozoic tectonic development of Greece and Albania in the context of alternative reconstructions of Tethys in the eastern Mediterranean region: International Geology Review, v. 54, n. 4, p. 373–454, http://dx.doi.org/10.1080/00206814.2010.543791

Robertson, A. H. F., Parlak, O., and Ustaömer, T., 2009, Mélange genesis and ophiolite emplacement related to subduction of the northern margin of the Tauride Anatolide continent, central and western Turkey, *in* van Hinsbergen, D. J. J., Edwards, M. A., and Govers, R., editors, Collision and collapse at the Africa–Arabia–Eurasia subduction zone: Geological Society, London, Special Publications, v. 311, p. 9–66, http://dx.doi.org/10.1144/SP311.2

Roddick, J. F., Cameron, W. E., and Smith, A. G., 1979, Permo-Triassic and Jurassic Ar–Ar ages from Greek ophiolites and associated rocks: Nature, v. 279, p. 788–790, http://dx.doi.org/10.1038/279788a0

Rolland, Y., Galoyan, G., Bosch, D., Sosson, M., Corsini, M., Fornari, M., and Verati, C., 2009a, Jurassic back-arc and hot-spot related series in the Armenian ophiolites—Implications for the obduction process: Lithos, v. 112, n. 3–4, p. 163–187, http://dx.doi.org/10.1016/j.lithos.2009.02.006

Rolland, Y., Billo, S., Corsini, M., Sosson, M., and Galoyan, G., 2009b, Blueschists of the Amasia–Stepanavan Suture Zone (Armenia): linking Tethys subduction history from E-Turkey to W-Iran: International Journal Earth Sciences, v. 98, n. 3, p. 533–550. http://dx.doi.org/10.1007/s00531-007-0286-8

Rolland, Y., Galoyan, G., Sosson, M., Melkonyan, R., and Avagyan, A., 2010, The Armenian ophiolite: insight for Jurassic back-arc formation, Lower Cretaceous hot spot magmatism and Upper Cretaceous obduction over the south Armenian block, *in* Sosson, M., Kaymakçı, N., Stephenson, R. A., Bergerat, F., and Starostenko, V., editors, Sedimentary basin tectonics from the Black Sea and Caucasus to the Arabian platform: Geological Society, London, Special Publications, v. 340, p. 353–382, http://dx.doi.org/10.1144/SP340.15

Rollinson, H. R., 1995, Using geochemical data: evaluation, presentation, interpretation: London, Longman Group Limited, 3rd Edition, 352 p.

——— 2008, The geochemistry of mantle chromitites from the northern part of the Oman ophiolite: inferred parental melt compositions: Contributions to Mineralogy and Petrology, v. 156, n. 3, p. 273–288, http://dx.doi.org/10.1007/s00410-008-0284-2

Sarıfakıoğlu, E., Özen, H., and Winchester, J. A., 2009, Petrogenesis of the Refahiye ophiolite and its tectonic significance for Neotethyan ophiolites along the İzmir-Ankara-Erzincan suture zone: Turkish Journal of Earth Sciences, v. 18, n. 2, p. 187–207.

Sarkarinejad, K., 2003, Structural and microstructural analysis of a palaeo-transform fault zone in the Neyriz ophiolite, Iran, *in* Dilek, Y., and Robinson, P. T., editors, Ophiolites in earth history: The Geological Society, London, Special Publication, v. 218, p. 129–145, http://dx.doi.org/10.1144/GSL.SP.2003.218.01.08

Schumacher, J. C., 1997, Appendix 2, The estimation of the proportions of ferric iron in electron microprobe analyses of amphiboles, *in* Leake, B. E., Woolley, A. R., Arps, C. E. S., Birch, W. D., Gilbert, M. C., Grice, J. D., Hawthorne, F. C., Kato, A., Kisch. H. J., Kirvovichev, V. G., Linthout, K., Laird, J., Mandarino, J. A., Maresch, W. V., Nickel, E. H., Rock, N. M. S., Schumacher, J. C. Smith, D. C., Stephenson, N. C. N., Ungaretti, L, Whittaker, E. J. W., and Youzhi, G., contributors, Nomenclature of amphiboles; report of the subcommittee on amphiboles of the International Mineralogical Association, Commission on New Minerals and Mineral Names: Canadian Mineralogist, v. 35, p. 238–246.

Searle, M., and Cox, J., 1999, Tectonic setting, origin, and obduction of the Oman ophiolite: Geological Society of America Bulletin, v. 111, n. 1, p. 104–122, http://dx.doi.org/10.1130/0016-7606(1999)111⟨0104:TSOAOO⟩2.3.CO;2

Şen, C., 2007, Jurassic volcanism in the eastern Pontides: is it rift related or subduction related?: Turkish Journal of Earth Sciences, v. 16, n. 4, p. 523–539.

Şengör, A. M. C., 1990, Plate-tectonics and orogenic research after 25 years: A Tethyan perspective: Earth Science Reviews, v. 27, n. 1–2, p. 1–201, http://dx.doi.org/10.1016/0012-8252(90)90002-D

Şengör, A. M. C., and Natal'in, B. A., 1996, Paleotectonics of Asia: fragment of a synthesis, *in* Yin, A., and Harrison, T. M., editors, The tectonics of Asia: New York, Cambridge University Press, p. 486–640.

——— 2004, Phanerozoic analogues of Archaean oceanic basement fragments: Altaid ophiolites and ophirags, *in* Kusky, T. M., editor, Precambrian ophiolites and related rocks: Developments in Precambrian geology, v. 13, p. 675–726, http://dx.doi.org/10.1016/S0166-2635(04)13021-1

Şengör, A. M. C., and Yılmaz, Y., 1981, Tethyan evolution of Turkey: a plate tectonic approach: Tectonophysics, v. 75, n. 3–4, p. 181–241, http://dx.doi.org/10.1016/0040-1951(81)90275-4

Şengör, A. M. C., Yılmaz, Y., and Ketin, I., 1980, Remnants of a pre-Late Jurassic ocean in northern Turkey: Fragments of Permian-Triassic Paleo-Tethys?: Geological Society of America Bulletin, v. 91, n. 10, p. 599–609, http://dx.doi.org/10.1130/0016-7606(1980)91⟨599:ROAPJO⟩2.0.CO;2

——— 1982, Remnants of a pre-Late Jurassic ocean in northern Turkey: Fragments of Permian-Triassic Tethys? Reply: Geological Society of America Bulletin, v. 93, p. 932–936, http://dx.doi.org/10.1130/0016-7606(1982)93⟨932:ROAPJO⟩2.0.CO;2

Şengör, A. M. C., Satır, M., and Akkök, R., 1984, Timing of tectonic events in the Menderes massif, western Turkey: Implications for tectonic evolution and evidence for Pan-African basement in Turkey: Tectonics, v. 3, n. 7, p. 693–707, http://dx.doi.org/10.1029/TC003i007p00693

Şengör, A. M. C., Tüysüz, O., İmren, C., Sakınç, M., Eyidoğan, H., Görür, N., Le Pichon, X., and Rangin, C., 2005, The North Anatolian Fault: a new look: Annual Review of Earth and Planetary Sciences, v. 33, p. 37–112, http://dx.doi.org/10.1146/annurev.earth.32.101802.120415

Shervais, J. W., 2001, Birth, death, and resurrection: The life cycle of suprasubduction-zone ophiolites: Geochemistry Geophysics Geosystems, v. 2, n. 1, http://dx.doi.org/10.1029/2000GC000080

Silver, E. A., and Reed, D. L., 2008, Backthrusting in accretionary wedges: Journal of Geophysical Research: Solid Earth, v. 93, B4, p. 3116–3126, http://dx.doi.org/10.1029/JB093iB04p03116

Sosson, M., Rolland, Y., Müller, C., Danelian, T., Melkonyan, R., Kekelia, S., Adamia, S., Babazadeh, V., Kangarlı, T, Avagyan, A., Galoyan, G., and Mosar, J., 2010, Subductions, obduction and collision in the Lesser Caucasus (Armenia, Azerbaijan, Georgia), new insights, *in* Sosson, M., Kaymakçı, N., Stephenson, R. A., Bergerat, F., and Starostenko, V., editors, Sedimentary basin tectonics from the black sea and the Caucasus to the Arabian platform: Geological Society, London, Special Publications, v. 340, p. 329–352, http://dx.doi.org/10.1144/SP340.1

Spray, J. G., Bébien, J., Rex, D. C., and Roddick, J. C., 1984, Age constraints on the igneous and metamorphic evolution of magmatism in the Hellenic–Dinaric ophiolites, *in* Dixon, J. E., and Robertson, A. H. F.,

editors, The Geological Evolution of the Eastern Mediterranean: Geological Society, London, Special Publications, v. 17, p. 619–627 http://dx.doi.org/10.1144/GSL.SP.1984.017.01.48
Stern, R. J., and Bloomer, S. H., 1992, Subduction zone infancy: Examples from the Eocene Izu-Bonin-Mariana and Jurassic Cafornia arcs: Geological Society of America Bulletin, v. 104, n. 12, p. 1621–1636, http://dx.doi.org/10.1130/0016-7606(1992)104⟨1621:SZIEFT⟩2.3.CO;2
Sun, S-s., and McDonough, W. F., 1989, Chemical and isotopic systematics of oceanic basalts: implications for mantle composition and processes, *in* Saunders, A. D., and Norry, M. J., editors, Magmatism in the oceanic basins: Geological Society, London, Special Publications, v. 42, p. 313–345, http://dx.doi.org/10.1144/GSL.SP.1989.042.01.19
Topuz, G., Altherr, R., Kalt, A., Satır, M., Werner, O., and Schwarz, W. H., 2004a, Aluminous granulites from the Pulur complex, NE Turkey: a case of partial melting, efficient melt extraction and crystallization: Lithos, v. 72, n. 3–4, p. 183–207, http://dx.doi.org/10.1016/j.lithos.2003.10.002
Topuz, G., Altherr, R., Satır, M., and Schwarz, W. H., 2004b, Low-grade metamorphic rocks from the Pulur complex, NE Turkey: implications for the pre-Liassic evolution of the Eastern Pontides: International Journal of Earth Sciences, v. 93, n. 1, p. 72–91, http://dx.doi.org/10.1007/s00531-003-0372-5
Topuz, G., Altherr, R., Schwarz, W. H., Dokuz, A., and Meyer, H.-P., 2007, Variscan amphibolite-facies metamorphic rocks from the Kurtoğlu metamorphic complex (Gümüşhane area, Eastern Pontides, Turkey): International Journal of Earth Sciences, v. 96, n. 5, p. 861–873, http://dx.doi.org/10.1007/s00531-006-0138-y
Topuz, G., Altherr, R., Siebel, W., Schwarz, W. H., Zack, T., Hasözbek, A., Barth, M., Satır, M., and Sen, C., 2010, Carboniferous high-potassium I-type granitoid magmatism in the Eastern Pontides: The Gümüshane pluton (NE Turkey): Lithos, v. 116, n. 1–2, p. 92–110, http://dx.doi.org/10.1016/j.lithos.2010.01.003
Topuz, G., Okay, A. I., Altherr, R., Schwarz, W. H., Siebel, W., Zack, T., Satır, M., and Şen, C., 2011, Post-collisional adakite-like magmatism in the Ağvanis Massif and implications for the evolution of the Eocene magmatism in the Eastern Pontides (NE Turkey): Lithos, v. 125, n. 1–2, p. 131–150, http://dx.doi.org/10.1016/j.lithos.2011.02.003
Topuz, G., Göçmengil, G., Rolland, Y., Çelik, Ö. F., Zack, T., and Schmitt A. K., 2012, Jurassic accretionary complex and ophiolite from northeast Turkey: No evidence for the Cimmerian continental ribbon: Geology, v. 41, p. 255–258, http://dx.doi.org/10.1130/G33577.1
Topuz, G., Okay, A. I., Altherr, R., Schwarz, W. H., Sunal, G., and Altınkaynak, L., 2013, Triassic subduction in northeast Turkey: Evidence from the Ağvanis metamorphic rocks: Island Arc.
Ustaömer, T., and Robertson, A. H. F., 2010, Late Palaeozoic-Early Cenozoic tectonic development of the Eastern Pontides (Artvin area), Turkey: stages of closure of Tethys along the southern margin of Eurasia, *in* Sosson, M., Kaymakçı, N., Stephenson, R. A., Bergerat, F., and Starostenko, V., editors, Sedimentary basin tectonics from the black sea and Caucasus to the Arabian platform: Geological Society, London, Special Publications, v. 340, p. 281–327, http://dx.doi.org/10.1144/SP340.13
Ustaömer, T., Robertson, A. H. F., Ustaömer, P. A., Gerdes, A., and Peytcheva, I., 2013, Constraints on Variscan and Cimmerian magmatism and metamorphism in the Pontides (Yusufeli–Artvin area), NE Turkey from U–Pb dating and granite geochemistry, *in* Robertson, A. H. F., Parlak, O., and Ünlügenç, U. C., editors, Geological Development of Anatolia and the Easternmost Mediterranean Region: Geological Society, London, Special Publications, v. 372, p. 49–74, http://dx.doi.org/10.1144/SP372.13
Ustaszewski, K., Schmid, S. M., Lugovic, B., Schuster, R., Schaltegger, U., Bernoulli, D., Hottinger, L., Kounov, A., Fügenschuh, B., and Schefer, S., 2009, Late Cretaceous intra-oceanic magmatism in the internal Dinarides (northern Bosnia and Herzegovina): Implications for the collision of the Adriatic and European plates: Lithos, v. 108, n. 1–4, p. 106–125, http://dx.doi.org/10.1016/j.lithos.2008.09.010
Ustaszewski, K., Kounov, A., Schmid, S. M., Schaltegger, U., Krenn, E., Frank, W., and Fugenschuh, B., 2010, Evolution of the Adria-Europe plate boundary in the northern Dinarides: From continent-continent collision to back-arc extension: Tectonics, v. 29, n. 6, TC6017, 34 p., http://dx.doi.org/10.1029/2010TC002668
Uysal, İ., Tarkian, M., Sadıklar, M. B., Zaccarini, F., Meisel, T., Garuti, G., and Heidrich, S., 2009, Petrology of Al- and Cr-rich ophiolitic chromitites from the Muğla, SW Turkey: implications from the composition of chromite, solid inclusions of platinum-group mineral, silicate and base-metal mineral, and Os-isotope geochemistry: Contributions to Mineralogy and Petrology, v. 158, n. 5, p. 659–674, http://dx.doi.org/10.1007/s00410-009-0402-9
Uysal, İ., Dilek, Y., Sarıfakıoğlu, E., and Meisel, T., 2010, Remnants of the Rheic SSZ oceanic lithosphere (320 Ma) within the Izmir-Ankara-Erzincan suture zone in NE Turkey: New geochemical and Re-Os isotope data from the Rehafiye-Erzincan Ophiolite: Vienna, European Geosciences Union(EGU) General Assembly 2010, p. 7170.
Vernon, R. H., 2000, Review of microstructural evidence of magmatic and solid-state flow: Electronic Geosciences (Visual Geosciences), v. 5, n. 2, 23 p., ISSN:1610-2924.
Vernon, R. H., and Collins, W. J., 2011, Structural criteria for identifying granitic cumulates: Journal of Geology, v. 119, n. 2, p. 127–142, http://dx.doi.org/10.1086/658198
von Huene, R., and Scholl, D. W., 1991, Observations at convergent margins concerning sediment subduction, subduction erosion, and the growth of continental crust: Reviews of Geophysics, v. 29, n. 3, p. 279–316, http://dx.doi.org/10.1029/91RG00969
Wakabayashi, J., 2013, Subduction initiation, subduction accretion and nonaccretion, large-scale material movement, and localization of subduction megaslip recorded in Franciscan complex and related rocks, California, *in* Putirka, K., editor, Geological excursions from Fresno, California and the Central valley: A Tour of California's Iconic Geology: Geological Society of America Field Guide, v. 32, p. 129–162, http://dx.doi.org/doi:10.1130/2013.0032(07)

Wakabayashi, J., and Dilek, Y., 2000, Spatial and temporal relationship between ophiolites and their metamorphic soles: A test of models of forearc ophiolite genesis, *in* Dilek, Y., Moores, E. M., Elthon, D., and Nicolas, A., editors, Ophiolites and oceanic crust: new insights from field studies and the ocean drilling program: Geological Society of America Special Papers, v. 349, p. 53–64, http://dx.doi.org/10.1130/0-8137-2349-3.53

——— 2003, What constitutes "emplacement" of an ophiolite?: Mechanisms and relationship to subduction initiation and formation of metamorphic soles, *in* Dilek, Y., and Robinson, R. T., editors., Ophiolites in Earth History: Geological Society, London, Special Publications, v. 218, p. 427–447, http://dx.doi.org/10.1144/GSL.SP.2003.218.01.22

Wakabayashi, J., Ghatak, A., and Basu, A. R., 2010, Suprasubduction-zone ophiolite generation, emplacement, and initiation of subduction: A perspective from geochemistry, metamorphism, geochronology, and regional geology: Geological Society of America Bulletin, v. 122, n. 9–10, p. 1548–1568, http://dx.doi.org/10.1130/B30017.1

Westbrook, G. K., 1982, The Barbados ridge complex: tectonics of a forearc system, *in* Leggett, J. K., editor, Trench-forearc geology: Sedimentation and tectonics on modern and ancient active plate margins: Geological Society, London, Special Publications, v. 10, p. 275–290, http://dx.doi.org/10.1144/GSL.SP.1982.010.01.18

Whattam, S. A., and Stern, R. J., 2011, The "subduction initiation rule": a key for linking ophiolites, intra-oceanic forearcs, and subduction initiation: Contributions to Mineralogy and Petrology, v. 162, n. 5, p. 1031–1045, http://dx.doi.org/10.1007/s00410-011-0638-z

Yılmaz, A., 1985, Yukarı Kelkit çayı ile Munzur dağları arasının temel jeoloji özellikleri ve yapısal evrimi: Türkiye Jeoloji Kurumu Bülteni, v. 28, n. 2, p. 79–92.

Yılmaz, A., and Yılmaz, H., 2004, Geology and structural evolution of the Tokat Massif (Eastern Pontides, Turkey): Turkish Journal of Earth Sciences, v. 13, p. 231–246.

Yılmaz, O., and Boztuğ, D., 1986, Kastomonu granitoids belt of northern Turkey: First arc plutonism product related to subduction of Paleo-Tethys: Geology, v. 14, n. 2, p. 179–183, http://dx.doi.org/10.1130/0091-7613(1986)14⟨179:KGBONT⟩2.0.CO;2